Mechanistic, Kinetic, and Process Investigation of Galactose Isomerization to Tagatose

by

Seyedamirreza Babaei

B.S., University of Tehran, 2024

A THESIS

submitted in partial fulfillment of the requirements for the degree

MASTER OF SCIENCE

Carl and Melinda Helwig Department of Biological and Agricultural Engineering
College of Carl R. Ice College of Engineering.

KANSAS STATE UNIVERSITY
Manhattan, Kansas

2026

Approved by:

Major Professor
Jikai Zhao

Copyright

Abstract

The increasing prevalence of obesity and metabolic disorders has intensified the demand for low-calorie sugar alternatives that maintain the sensory properties of sucrose. D-Tagatose, a rare ketohexose derived from D-galactose, possesses approximately 92% of the sweetness of sucrose while providing significantly lower caloric value (1.5 kcal g^{-1}) and an extremely low glycemic index (3). Despite these advantages, large-scale production of tagatose remains limited by inefficient conversion processes and an incomplete understanding of the reaction pathways governing galactose isomerization. This thesis investigates the conversion of galactose to tagatose through CaO-mediated alkaline systems and develops a kinetic and thermodynamic framework to describe the underlying reaction network.

In the first part of this work, a CaO-mediated reaction system was investigated for the isomerization of galactose under mild aqueous conditions. Using a 0.5 M galactose solution with a CaO/galactose molar ratio of 1/1, the reaction achieved 86.65% galactose conversion with 50.47% tagatose selectivity after 30 min, corresponding to a tagatose yield of 43.73%. Mechanistic observations indicate that CaO primarily acts as a source of hydroxide ions that initiate the formation of enediol intermediates responsible for aldose–ketose rearrangement. Subsequent coordination between Ca^{2+} species and galactose hydroxyl groups may further influence reaction pathways and product distribution. Process evaluation of the system indicated a minimum selling price of approximately \$0.80–0.85 kg^{-1}, depending on the neutralization strategy, while life-cycle assessment showed that CO_2 neutralization reduced the global warming potential to approximately 0.90 kg CO_2-eq kg^{-1} of tagatose.

The second part of this study examines the kinetics and thermodynamics of galactose isomerization using a homogeneous triethylamine system to isolate the intrinsic reaction behavior. Experiments conducted between 40 and 100 °C were described using a reversible reaction network involving galactose, tagatose, and talose together with irreversible degradation pathways. The forward rate constant for galactose-to-tagatose conversion increased from 2.44×10^{-5} to 4.58×10^{-4} min^{-1} across the studied temperature range. Arrhenius analysis yielded activation energies of 50.6 kJ mol^{-1} for the galactose–tagatose isomerization step and 73.1 kJ mol^{-1} for the tagatose–talose epimerization pathway. Thermodynamic analysis indicated that the isomerization reactions are endothermic and entropy-driven, with equilibrium strongly influenced by temperature.

Overall, this work provides new insights into the reaction pathways, kinetics, and process performance of galactose isomerization to tagatose. By integrating reaction system development, kinetic modeling, techno-economic analysis, and life-cycle assessment, this study establishes a framework for improving the efficiency and sustainability of rare sugar production.

Table of Contents

List of Figures

List of Tables

Chapter 1 - Literature Review

Portions of this chapter were adapted from the following publication: Babaei, S., et al. “A Critical Review of Catalytic Glucose-to-Fructose Isomerization”, ChemistrySelect, 2025, 10, 48, Doi.org/10.1002/slct.202505344. The author of this thesis served as the first author of the publication and was primarily responsible for literature analysis, manuscript preparation, and synthesis of the reviewed catalytic systems.

1.1 Introduction

Excessive consumption of caloric sweeteners has become a major global health concern over the past several decades.[1] According to the World Health Organization, global sugar intake has increased substantially, with average daily consumption in many developed countries exceeding 100 g per person.[2] High dietary sugar intake has been strongly associated with the rising prevalence of metabolic disorders such as obesity, type 2 diabetes, and cardiovascular diseases.[3–5] In the United States alone, the prevalence of diabetes among adults has increased from approximately 5.5 % in the early 1980s to more than 11 % in recent years.[6] These health concerns have driven significant interest in identifying alternative sweeteners that provide desirable sensory properties while reducing caloric intake and glycemic impact.[7] Among the various candidates, rare sugars have attracted increasing attention due to their unique metabolic characteristics and potential applications in functional foods and nutraceutical formulations.[8–10]

D-Tagatose is one of the most promising rare sugars due to its favorable nutritional and functional properties. Structurally, tagatose is a ketohexose that is the C-4 epimer of D-fructose and can be produced through isomerization of D-galactose.[11–13] Tagatose possesses approximately 92 % of the sweetness of sucrose while providing significantly lower caloric value, estimated at about 1.5 kcal g^{-1} compared to 4 kcal g^{-1} for sucrose.[14–16] In addition, tagatose

exhibits a low glycemic index (GI ≈ 3), making it particularly attractive for diabetic and low-glycemic diets.[17] Beyond its sweetness, tagatose has been reported to exhibit prebiotic effects and potential benefits in regulating blood glucose levels.[18] These characteristics have generated increasing interest in the food and pharmaceutical industries, where tagatose is considered a promising ingredient for low-calorie sweeteners, functional foods, and nutraceutical formulations.[19,20] However, the widespread industrial adoption of tagatose remains limited due to challenges associated with efficient and sustainable production processes.

Industrial production of D-tagatose primarily relies on the isomerization of D-galactose, an aldose sugar that can be obtained from lactose hydrolysis or other biomass-derived carbohydrate streams. The transformation of galactose into tagatose involves an aldose–ketose isomerization reaction, in which the carbonyl group shifts from the C-1 position to the C-2 position through the formation of an enediol intermediate. This rearrangement can occur under catalytic conditions and represents a fundamental reaction pathway in carbohydrate chemistry. However, the reaction is thermodynamically limited and often accompanied by side reactions such as sugar degradation, epimerization, and formation of colored byproducts. As a result, achieving high conversion and selectivity toward tagatose remains a significant challenge in the development of efficient catalytic processes. Understanding the reaction pathways and factors governing the isomerization equilibrium is therefore essential for improving the production efficiency of tagatose from galactose.

Several catalytic strategies have been investigated for the isomerization of galactose to D-tagatose, including enzymatic, homogeneous, and heterogeneous catalytic systems. Enzymatic processes using L-arabinose isomerase have demonstrated tagatose yields typically ranging from 30–50% under optimized conditions, but these systems often require elevated temperatures (50–

70 °C) and exhibit limited operational stability. Homogeneous base catalysts have also been explored for chemical isomerization. For example, organic bases such as triethylamine and arginine have been reported to promote galactose isomerization, achieving conversions of approximately 40–60% with tagatose selectivities between 50–70% depending on reaction conditions. In addition, heterogeneous catalytic systems including Sn-β zeolites, hydrotalcite-derived materials, and alkaline earth metal oxides have been investigated to improve catalyst stability and facilitate product separation. For instance, Lewis acidic Sn-β catalysts have been shown to catalyze aldose–ketose isomerization through hydride-shift mechanisms, while basic metal oxides such as CaO and MgO can promote isomerization via base-catalyzed enediol pathways. Despite these advances, many catalytic systems still face limitations such as incomplete conversion, side-reaction formation, and challenges in achieving both high selectivity and process sustainability.

Despite significant progress in catalytic sugar isomerization, several challenges remain in achieving efficient and sustainable production of D-tagatose. Many reported catalytic systems suffer from limited selectivity, thermodynamic equilibrium constraints, and the formation of undesired degradation products during the isomerization process. In addition, the fundamental kinetic and thermodynamic behavior governing galactose–tagatose interconversion remains insufficiently understood, which complicates reactor design and process optimization for large-scale production. Addressing these challenges requires both the development of effective catalytic systems and a deeper understanding of the reaction kinetics and equilibrium characteristics. Therefore, this thesis investigates the catalytic conversion of galactose to D-tagatose using CaO-mediated reaction systems under mild conditions, followed by a detailed kinetic and thermodynamic analysis of the galactose isomerization reaction. The findings presented in the

following chapters aim to contribute to the development of more efficient catalytic processes for sustainable rare sugar production.

1.2 Mechanisms of Galactose-Tagatose Isomerization

The isomerization of aldose sugars to their corresponding ketoses is commonly described by the Lobry de Bruyn–van Ekenstein transformation, a base-catalyzed rearrangement that proceeds through the formation of an enediol intermediate (**Figure 1-1**).[21] Under alkaline conditions, a base abstracts a proton adjacent to the carbonyl group of the aldose molecule, generating a reactive sugar anion. This deprotonation allows electron delocalization between the C-1 and C-2 atoms, resulting in the formation of an enediol structure. Subsequent protonation of this intermediate at different carbon positions enables the rearrangement of the carbonyl group, thereby converting an aldose sugar into its corresponding ketose. In the case of galactose, this pathway facilitates the transformation into tagatose and other related ketose or epimeric products, making the enediol-mediated rearrangement a fundamental step in galactose–tagatose isomerization reactions.[22]

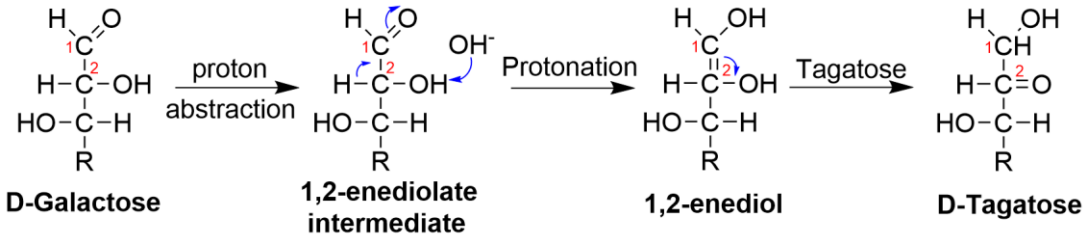

Figure 1-1. Base-catalyzed Lobry de Bruyn–van Ekenstein rearrangement of D-galactose to D-tagatose via a 1,2-enediol intermediate.

In aqueous alkaline environments, the isomerization of galactose typically proceeds through a base-catalyzed pathway involving sequential proton transfer steps. The reaction begins with the abstraction of a proton from the C-2 position of the cyclic galactose molecule, which generates a galactose anion and initiates the opening of the sugar ring. This process leads to the

formation of a 1,2-enediol intermediate, a key transient species that enables rearrangement of the carbonyl group within the carbohydrate framework. Following the formation of this intermediate, protonation at different positions can produce multiple products. Protonation at the C-2 carbon results in the formation of D-tagatose, whereas protonation at alternative positions may yield epimeric sugars such as D-talose. Because these transformations occur through the same enediol intermediate, several isomeric sugars may form simultaneously, and the product distribution is strongly influenced by reaction conditions such as pH, temperature, and catalyst strength.[23]

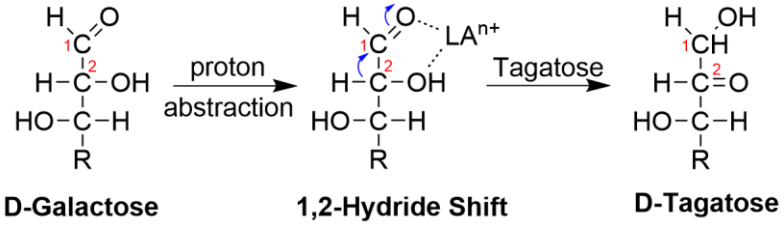

Figure 1-2. Lewis-acid-catalyzed (LA) mechanism for D-galactose isomerization to D-tagatose via a 1,2-hydride shift.

In addition to base-catalyzed pathways, aldose–ketose isomerization can also occur through Lewis acid catalysis, which proceeds via a fundamentally different mechanism (**Figure 1-2**).[24] In this pathway, the sugar molecule coordinates to a Lewis acidic metal center, typically associated with catalysts such as Sn-containing zeolites or other metal-based materials. The coordination of the hydroxyl groups to the metal site stabilizes the transition state and facilitates an intramolecular hydride shift between the C-1 and C-2 carbon atoms.[25–27] Unlike the base-catalyzed route that involves enediol formation, the Lewis-acid mechanism proceeds through a cyclic transition state that directly rearranges the carbonyl position. This hydride transfer mechanism has been widely reported in heterogeneous catalytic systems and often exhibits improved selectivity under controlled conditions. However, similar to base-catalyzed reactions, competing side reactions and thermodynamic limitations can still affect product distribution,

highlighting the importance of catalyst design and reaction condition optimization in aldose–ketose isomerization processes.[28]

1.3 Non-enzymatic Systems for Galactose-Tagatose Isomerization

Table 1. Isomerization of Galactose to Tagatose in the Presence of Different Chemicals

Chemical	Galactose Concentration	pH	Temperature (°C)	Time	Tagatose Selectivity (%)	Galactose Conversion (%)	Tagatose Yield (%)	Ref
KOH	n/a	11.5	25	2 weeks	n/a	n/a	15	[29]
$MgO.Al_2O_3$	0.11 mol/L	8.95-9.55	110	2 h	43-56	21-25	18-27	[22]
Supercritical ethanol	0.5 wt%	n/a	180	500 s	>70	32	24	[30]
Sn/β	10 wt%	2.6	110	1 h	83	29	24	[22]
Sn/deAl-β	10 wt%	n/a	110	2 h	90	31	28	[31]
triethylamine/boric acid	25 g/L	11	70	3 h	n/a	n/a	34	[32]
$CaCl_2$, triethylamine	1 mM/L	6.5	60	10 min	n/a	n/a	34	[33]
$NaAlO_2$	1.6% (w/v)	n/a	40	9 h	n/a	n/a	>60	[34]
$CaCl_2$, CaO	0.1 kg/L	12.5	20	1.5 h	n/a	n/a	72	[35]
$Ca(OH)_2$	1 M/L	n/a	<20	2 h	n/a	n/a	92	[36]

$MgBr_2$	n/a	n/a	120	60 min	73	30	22	[37]
anion exchange resin	5-10 wt%	8-9	60-80	2-4 h	n/a	n/a	20	[38]
arginine	5% (w/v)	10	120	20 min	68	25	17	[39]

n/a: not available

The earliest non-enzymatic studies relied on strongly alkaline media to promote the Lobry de Bruyn–van Ekenstein rearrangement of galactose (**Table 1**). Simple homogeneous bases such as KOH were shown to convert galactose to tagatose at room temperature; however, the reaction proceeded extremely slowly. For example, under alkaline conditions at pH 11.5 and 25 °C, approximately two weeks were required to obtain a tagatose yield of only about 15 %. Such low productivity reflects the intrinsic limitations of simple alkaline systems, where the formation of the enediol intermediate occurs slowly and prolonged exposure to basic conditions promotes competing sugar degradation reactions.[29]

To improve reaction rates, heterogeneous basic materials have been investigated as alternatives to simple homogeneous bases. Mixed oxide catalysts such as $MgO–Al_2O_3$ have been reported to facilitate galactose isomerization at elevated temperatures around 110 °C. Under these conditions, galactose concentrations of approximately 0.11 mol L^{-1} produced galactose conversions between 21 and 25 % with tagatose selectivities ranging from 43 to 56 % after about 2 h of reaction, corresponding to tagatose yields of 18–27 %.[22] The enhanced performance of these materials is commonly attributed to accessible basic sites on the oxide surface that promote

formation of the enediol intermediate and accelerate aldose–ketose rearrangement relative to homogeneous alkaline systems.

In addition to basic catalysts, several studies have explored alternative reaction environments capable of promoting sugar isomerization. Supercritical ethanol has been investigated as a high-temperature reaction medium, where galactose solutions containing approximately 0.5 wt % substrate were treated at around 180 °C for short residence times of about 500 s. Under these conditions, galactose conversion of roughly 32 % and tagatose yields near 24 % were reported.[30] Although such high-temperature solvent systems can significantly accelerate reaction kinetics, the severe operating conditions limit their practical applicability for large-scale production.

Lewis-acid-based materials have also attracted attention because they promote isomerization through a different mechanistic pathway involving hydride transfer rather than the classical enediol mechanism. For example, Sn-β zeolite catalysts have been reported to achieve tagatose selectivities as high as 83 % at temperatures near 110 °C with galactose conversions around 29 %.[22] Further modification of the zeolite framework, such as dealuminated Sn-β materials, has led to improved selectivity approaching 90 % with conversions near 31 %, corresponding to tagatose yields of approximately 28 %.[31] These systems illustrate the potential advantages of Lewis-acid sites in controlling reaction selectivity, although catalyst synthesis and stability remain important considerations.

More recent studies have also investigated homogeneous organic bases and alkaline salt systems. Combinations such as triethylamine with boric acid have been shown to produce tagatose yields around 34 % at approximately 70 °C,[32] while systems containing $CaCl_2$ with triethylamine have demonstrated similar yields under milder conditions.[33] Other alkaline

reagents, including $NaAlO_2$, have achieved tagatose yields exceeding 60 % at moderate temperatures,[34] suggesting that strong basic environments can significantly enhance reaction efficiency when degradation reactions are controlled.

Calcium-based systems represent another class of promising reaction media for galactose isomerization. In particular, combinations of $CaCl_2$ and CaO have been reported to produce tagatose yields up to 72 % under alkaline conditions,[35] while reactions involving $Ca(OH)_2$ have achieved yields approaching 92 % at temperatures below 20 °C.[36] These results highlight the strong influence of calcium species on the galactose–tagatose transformation, likely due to their ability to generate alkaline conditions while simultaneously interacting with carbohydrate hydroxyl groups. Such observations have motivated further investigation into calcium-mediated reaction systems for efficient rare-sugar production.

Additional reaction systems have also been explored, including $MgBr_2$, which produced tagatose selectivity of approximately 73 % with 30 % galactose conversion at 120 °C,[37] as well as ion-exchange resins and amino-acid-based promoters such as arginine.[38,39] While these systems demonstrate the broad range of chemical approaches available for promoting galactose isomerization, many still suffer from moderate yields or demanding reaction conditions. Consequently, developing reaction systems that combine high conversion, high selectivity, and mild operating conditions remains a central challenge in the non-enzymatic production of tagatose.

1.4 Future Perspective

The literature on galactose-to-tagatose conversion reveals a wide diversity of chemical systems capable of promoting aldose–ketose isomerization, yet several fundamental limitations remain before these approaches can be translated into robust industrial processes.[28] Many reported non-enzymatic systems require either strongly alkaline environments, elevated

temperatures, or long reaction times to achieve moderate yields. Under such conditions, competing degradation pathways, including sugar fragmentation, caramelization, and epimerization, can significantly reduce selectivity and complicate downstream purification.[40] Although certain systems, particularly those involving calcium species or Lewis-acid frameworks, have demonstrated promising tagatose yields, the underlying reaction mechanisms and the factors governing selectivity remain only partially understood. A deeper mechanistic understanding of the galactose–tagatose transformation is therefore essential for rationally improving reaction efficiency and minimizing undesired side reactions.[28]

Another important research need lies in the development of comprehensive kinetic and thermodynamic descriptions of the reaction network.[41] Many studies report conversion and yield data but lack detailed kinetic analysis capable of describing the reversible interconversion among galactose, tagatose, and other sugar isomers such as talose, as well as the parallel degradation reactions that occur under alkaline conditions.[42] Without quantitative kinetic models, it is difficult to identify optimal operating windows or predict reactor performance at larger scales. Future research should therefore focus on developing mechanistic reaction models that integrate experimental data with thermodynamic analysis to better understand equilibrium limitations, reaction pathways, and temperature effects in the galactose isomerization system.

Beyond reaction chemistry, the economic and environmental performance of emerging tagatose production technologies remains largely unexplored.[43] While numerous catalytic and chemical systems have been reported at laboratory scale, relatively few studies have evaluated their techno-economic feasibility or environmental impacts. For industrial implementation, it is essential to assess factors such as raw material consumption, reagent recovery, energy requirements, and downstream separation costs.[44] Techno-economic analysis (TEA) can

provide insight into the minimum selling price of tagatose and identify the key process variables that influence economic viability. At the same time, life-cycle assessment (LCA) is necessary to evaluate environmental indicators such as global warming potential, energy intensity, and resource utilization associated with different process configurations. Integrating TEA and LCA with reaction system development will be critical for guiding future research toward scalable and sustainable rare-sugar production technologies.

Addressing these challenges requires a combined approach that integrates reaction system development, mechanistic investigation, and process-level evaluation. In this context, the present thesis investigates galactose isomerization through CaO-mediated reaction systems and develops a kinetic and thermodynamic framework to describe the underlying reaction pathways. In addition, techno-economic analysis and life-cycle assessment are applied to evaluate the feasibility and sustainability of tagatose production processes. By bridging fundamental reaction chemistry with process analysis, this work aims to provide new insights that support the development of efficient and sustainable strategies for industrial D-tagatose production.

1.5 Conclusion

The non-enzymatic conversion of galactose to D-tagatose has attracted significant attention as a promising route for producing low-calorie rare sugars. Previous studies have demonstrated that a wide range of chemical systems—including homogeneous bases, mixed metal oxides, Lewis-acid zeolites, and calcium-based alkaline media—can promote the aldose–ketose isomerization reaction. However, the reported performance of these systems varies widely, with many processes achieving only moderate tagatose yields or requiring severe reaction conditions such as high temperatures, long reaction times, or strongly alkaline environments. These limitations arise from the complex reaction network governing galactose transformation, where

the desired galactose–tagatose isomerization competes with side reactions including epimerization and sugar degradation.

Although significant progress has been made in identifying chemical systems capable of promoting galactose isomerization, important challenges remain. In particular, mechanistic understanding of the reaction pathways, quantitative kinetic descriptions of the reaction network, and comprehensive assessments of process feasibility are still limited in the current literature. Addressing these knowledge gaps is essential for developing efficient and sustainable technologies for rare-sugar production. Therefore, the following chapters of this thesis investigate galactose isomerization through CaO-mediated reaction systems and develop a detailed kinetic and thermodynamic framework for the galactose–tagatose transformation, together with techno-economic and life-cycle evaluations of the proposed production process.

Chapter 2 - CaO-Mediated Production of D-Tagatose from Galactose

Portions of this chapter have been published previously in the following article: Babaei, S., et al. “Sustainable Production of Low-Calorie Tagatose via CaO-Promoted Galactose Isomerization with CO_2 Neutralization under Mild Conditions,” Industrial & Engineering Chemistry Research, 2.25, 38, 18656-18663, Doi.org/10.1021/acs.iecr.5c01664. The author of this thesis was the first author of the publication and was primarily responsible for experimental design, data analysis, and manuscript preparation.

2.1. Introduction

Obesity is a critical health issue both in the U.S. and globally, with alarming trends emerging over the past few decades. According to the most recent data (2017-2018), 42% of adults in the world are classified as obese, with 9% falling into the category of severe obesity.[45] This represents a significant rise from the 1980s when only 3% of adults were severely obese. The epidemic has also affected children, with nearly 1 in 5 adolescents (ages 5-19) considered obese as of 2022. Globally, obesity has been on a parallel trajectory.[46] By 2022, approximately 2.5 billion adults were classified as overweight, including 890 million who were obese. Childhood obesity is similarly alarming, with 160 million adolescents worldwide facing this condition.[47] Notably, low- and middle-income countries are experiencing a more rapid increase, and by 2035, 79% of the world's obese population is expected to reside in these regions.[48] The health consequences of this epidemic are profound, contributing to a marked rise in chronic conditions such as diabetes, cardiovascular disease, and cancer.[3–5] These are the direct results of an imbalance between calorie intake and energy use, aggravated by the widespread availability of high-calorie, nutrient-poor foods and increasingly sedentary lifestyles.[49–51]

The use of low-calorie sugars has garnered significant interest due to their potential to facilitate a reduction in individuals' overall caloric consumption, hence leading to weight loss.[52–54] The market for allulose (0.4 kcal/g), a low-calorie sugar alternative, has been expanding rapidly, driven by growing consumer awareness around health concerns like obesity and diabetes. In 2023, the global allulose market was valued at $128 million, with projections estimating a compound annual growth rate of 15%, leading to a market size of $440 million by 2032.[55] This growth reflects the rising demand for healthier, low-calorie sweeteners, particularly among keto and diabetic diets, as allulose minimizes blood sugar levels.[56] Despite this promising trend, allulose selling prices are high ($3.42/kg).[57] This cost burden limits consumer access and is a key barrier to broader market adoption. Additionally, allulose has only about 70% of the sweetness of sucrose, meaning larger quantities are required to match the sweetness level in food products. It can complicate formulation and affect the texture of various products. These findings suggest that low-cost, low-calorie sweeteners with a taste similar to sucrose are essential in addressing the obesity epidemic.

Tagatose has a far lower glycemic index (3 vs. 65) and caloric value (1.5 vs. 4 kcal/g) than sucrose and offers around 90% of the sweetness of sucrose.[14,28,58] Therefore, it could be an ideal choice for individuals with diabetes and aids in weight management. Importantly, tagatose has been approved for use in various food and beverage products as a "generally recognized as safe (GRAS)" ingredient.[59] The growing global demand for tagatose has prompted an increasing exploration of its production methods.[60] Lactose from whey (a byproduct in the dairy industry) can be split into glucose and galactose using lactase or acids. Research on the enzymatic isomerization of galactose to tagatose, facilitated by L-arabinose isomerases, is of great interest.[61–68] However, it encounters several challenges, including the poor thermal stability of

the enzymes, the low galactose conversion, and the lengthy processing time required.[28] In addition, research on the chemical and catalytic isomerization of galactose to tagatose is still in its infancy, with less than a dozen studies conducted using supercritical fluids,[30,69,70] hydrotalcite,[71,72] triethylamine,[32] arginine,[39] Sn-β zeolite,[22,31] boronate affinity,[73] and calcium hydroxide.[35,36] Overall, the tagatose selectivity and yield were often lower than 50% and 34%.[28] Orochem has previously patented and designed a process to produce tagatose from lactose using CaO.[74] In our previous study,[75] we found that CaO could effectively isomerize galactose to tagatose with a gel complex formed at room temperature. The complex was then neutralized with H_2SO_4 to produce tagatose and $CaSO_4$. Interestingly, galactose conversion almost had a linear relationship with CaO/galactose molar ratio, but the tagatose selectivity varied between 32% and 72% after 40 min of reaction without any discernible trend. Herein, we hypothesize that using CO_2 for neutralization might help improve tagatose selectivity and stabilize galactose conversion. Furthermore, utilizing CO_2 to neutralize $Ca(OH)_2$ may offer a potential route to reduce environmental impacts by forming $CaCO_3$, which can be easily filtered from the solution.

This study aims to demonstrate how reaction conditions (such as galactose concentration, CaO/galactose molar ratio, and reaction time) affect galactose conversion and tagatose selectivity. We investigated the roles of CaO (Ca^{2+} and OH^-) by substituting it with $CaCl_2$, triethylamine, arginine, or MgO. We then conducted a techno-economic analysis (TEA) and life-cycle assessment (LCA) of tagatose production involving the isomerization of galactose with CaO, followed by neutralization using CO_2, H_2SO_4, or H_3PO_4. This study proposes a cost-effective and environmentally friendly approach to produce tagatose from galactose.

2.2. Experimental Section

2.2.1 Tagatose synthesis

The desired amount of CaO, MgO, $CaCl_2$, triethylamine, or arginine was added to a beaker containing 50 mL of galactose (0.1-0.5 M) solution. The beakers were placed above the magnetic stirrer at 400 rpm for the desired reaction time at room temperature. In the case of CO_2 neutralization, the solution with a gel complex was then transferred into a carbonation machine (SodaStream International Ltd., United Kingdom) container for neutralization with CO_2 gas. When H_2SO_4 or H_3PO_4 was used for neutralization, the concentrated H_2SO_4 or H_3PO_4 was added drop by drop to the beakers. The pH of the resulting solution containing precipitate was usually around 6-7. $CaCO_3$, $CaSO_4$, or $Ca_3(PO4)_2$ precipitate was removed with a 0.2 μm VMR brand membrane. The liquid samples were diluted fivefold with HPLC-grade water before compositional analysis. Galactose and tagatose concentrations were measured with an Agilent 1200 HPLC coupled with a Refractive Index Detector and a Rezex RCM-Monosaccharide column (Phenomenex, Torrance, CA). HPLC water with a flow rate of 0.6 ml/min was used as the mobile phase, while the column temperature was maintained at 80 °C. Galactose conversion (%), tagatose selectivity (%), and tagatose yield (%) were calculated according to our previous study (eqs 1-3).[75]

$$Galactose\ conversion = \frac{[initial\ galactose\ concentration]-[final\ galactose\ concentration]}{[initial\ galactose\ concentration]} \times 100\% \quad (1)$$

$$Tagatose\ selectivity = \frac{[final\ galactose\ concentration]}{[initial\ galactose\ concentration]-[final\ galactose\ concentration]} \times 100\% \quad (2)$$

$$Tagatose\ yield = \frac{[final\ galactose\ concentration]}{[initial\ galactose\ concentration]} \times 100\% \quad (3)$$

2.2.2 Techno-economic analysis

The experimental data were utilized to construct a process model capable of processing 33,000 MT of galactose (0.5 M) solution annually. This equates to a processing capacity of 100 MT per day with an operation of 7,920 hours or 330 days per year. The isomerization reaction occurred in a stirred semicontinuous batch reactor with a vessel volume of 2,080 L and a flow rate of about 101.56 MT/day based on the scenarios. After 30 min of reaction, CO_2, H_2SO_4, or H_3PO_4 was injected into the reactor to neutralize the gel complex. The resulting slurry was pumped to a rotary vacuum filter to remove $CaCO_3$, $CaSO_4$, or $Ca_3(PO4)_2$ precipitate. After that, the tagatose-rich solution underwent simulated moving bed chromatography to separate galactose and tagatose. The galactose solution and tagatose solution were individually dried in tray dryers, with galactose and water being recycled back into the reaction system, and tagatose remained the sole product for sale. The technical data primarily consisted of mass and energy balances for all streams, which determined equipment capacities and energy consumption. Based on our experimental findings, these data were mainly derived from a rigorous and comprehensive process model developed using SuperPro Designer (Intelligen Inc., Scotch Plains, NJ, 2017). The capital expenditures (CAPEX) and operating expenses (OPEX) were evaluated for three scenarios, namely, isomerization of galactose with CaO (CaO/galactose molar ratio of 1/1) followed by neutralization with CO_2, H_2SO_4, or H_3PO_4. The minimum selling price (MSP) of tagatose was determined using a discounted cash flow rate of return (DCFROR) analysis (eqs. 4-5). The MSP indicator indicates the tagatose selling price at which the net present value (NPV) becomes zero based on the assumptions. A sensitivity analysis with a 50% increase and a 50% decrease in the factors was further conducted to reveal their influence on the MSP of tagatose.

$$PVAF = \frac{1-(1+r)^{-T}}{r} \quad (4)$$

$$MSP = \frac{(\frac{CAPEX}{PVAF} + OPEX \times (1-t) - \frac{CAPEX \times t}{T})}{Q \times (1-t)} \quad (5)$$

The MSP of tagatose is calculated based on eqs. 4-5, where PVAF is the present value annuity factor, r is the discount rate, T is the project lifespan, CAPEX is the total capital expenditure, OPEX is the annual operating cost, t is the tax rate, and Q is the annual production quantity.

2.2.3 Life cycle assessment

A cradle-to-grave LCA was performed to evaluate the environmental impacts of the three scenarios for producing tagatose from galactose adhering to the ISO 14040 series standards.[76] 46,47 The system boundary consisted of the isomerization reaction, neutralization, precipitate filtration, tagatose separation, and distillation sections. The functional unit was chosen as 1 kg of tagatose. The mass and energy balance data from TEA were used to create the foreground life cycle inventory (LCI) data. For the life cycle impact assessment (LCIA), the Tool for the Reduction and Assessment of Chemical and Other Environmental Impacts (TRACI) Version 2.1, developed by the U.S. Environmental Protection Agency, was employed to evaluate the cradle-to-grave environmental impacts. Eight ecological impact categories were considered, including global warming potential (GWP, kg CO_2-eq), acidification (AC, kg SO_2-eq), eutrophication (EU, kg N-eq), fossil fuel depletion (FFD, MJ), smog formation (SM, kg O_3-eq), human health non-carcinogenic (HHnc, Comparative Toxic Units for humans-CTUh), ecotoxicity (ET, Comparative Toxic Units for ecosystems-CTUe), and respiratory effects (RE, kg PM2.5-eq).

2.3. Results and Discussion

2.3.1 Tagatose synthesis with CaO and CO_2 neutralization

The isomerization of galactose (0.2 M) to tagatose using CaO for 30 min exhibits a notable influence of the CaO/galactose molar ratio on both galactose conversion and tagatose selectivity (**Figure 2-1a**). As the molar ratio increased from 1/10 to 1/1, galactose conversion exhibited a significant rise from 2.81% to 77.65%. However, tagatose selectivity exhibited a slightly different trend, increasing from 50.21% at a 1/10 ratio to 71.06% at a 1/2 ratio before declining to 57.77% at a 1/1 ratio. The highest yield of 44.86% was achieved at a CaO/galactose molar ratio of 1/1. Other products besides tagatose likely include mannose and talose via epimerization pathways and possibly small amounts of degradation byproducts such as organic acids or $Ca(OH)_2$ residues. At a CaO/galactose ratio of 1/1, the galactose conversion increased from 56.21% to 83.79% as the reaction time increased from 10 to 60 min (**Figure 2-1b**). The tagatose selectivity ranging from 58.88% to 62.82% was relatively constant. With a fixed CaO/galactose molar ratio of 1/1 and a reaction time of 30 min (**Figure 2-1c**), galactose conversion increased from 69.23% to 86.65% with the elevation of galactose concentration (0.1-0.5 M), indicating that higher galactose availability in water enhances the extent of reaction, likely due to more effective interaction with $Ca(OH)_2$. Conversely, tagatose selectivity decreased from 60.16% to 50.47%, suggesting that side reactions or degradation pathways become more prominent at elevated galactose concentrations. A yellowish hydrogel was formed with a CaO/galactose molar ratio of 1:1 after 30 min. The viscosity of the gel increased with an increase in galactose concentration. When the gel complex was neutralized with CO_2, it became liquid with a gray color. However, for 1 M galactose, the gel became significantly more rigid and cohesive, likely due to enhanced crosslinking between galactose molecules and Ca^{2+} ions. This dense network structure prevented CO_2 from fully diffusing into the gel, rendering neutralization ineffective. It is worth noting that CO_2 neutralization was achieved using a commercial soda machine operating at a relatively lower

working pressure of approximately 30–50 psi. For future research, employing higher-pressure or larger-scale CO_2 delivery systems with blending techniques may help penetrate and break down the gel complex for high galactose concentration solutions.

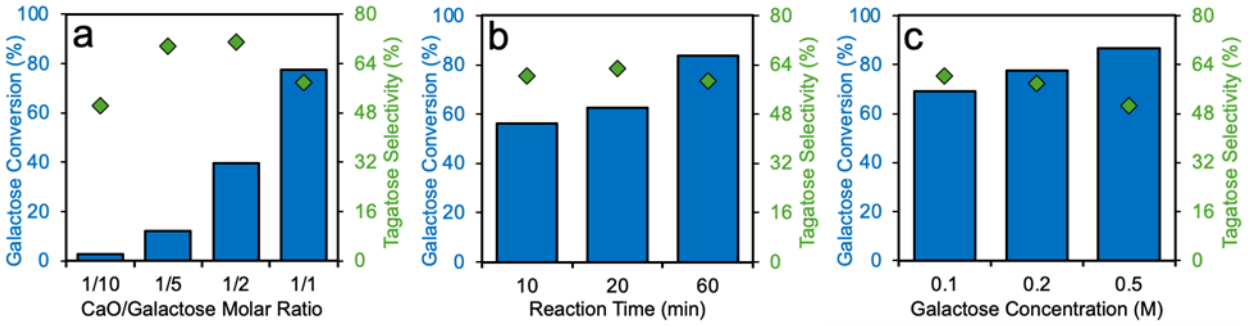

Figure 2-1. Effects of CaO/galactose molar ratio (a), reaction time (b), and galactose concentration (c) on galactose conversion and tagatose selectivity.

2.3.2 The role of CaO in galactose isomerization to tagatose

We conducted the isomerization of galactose (0.1-0.5 M) to tagatose with MgO/galactose molar ratio of 1/1 with subsequent CO_2 neutralization at room temperature (**Figure 2-2a**). Galactose conversion increased slightly but remained very low (2.87–9.39%) across varying galactose concentrations (0.1–0.5 M). Tagatose selectivity reached a maximum of 22.91% at 0.2 M galactose before declining to 16.66% at 0.5 M. This demonstrates that MgO is not selective for tagatose production. Other products that were observed besides tagatose include organic acids or $Mg(OH)_2$ residues.

We further investigated the role of Ca^{2+} by replacing CaO with $CaCl_2$ and evaluating the impact on galactose conversion and tagatose selectivity (**Figure 2-2b**). The combination of 0.1 M $CaCl_2$ with 0.4 M CaO achieved the highest galactose conversion (82.82%) and a tagatose selectivity of 52.57%. Increasing $CaCl_2$ to 0.2 M and 0.3 M while reducing CaO resulted in lower conversions (75.84% and 46.25%, respectively), though the 0.3 M CaCl2 + 0.2 M CaO condition

exhibited a notably higher tagatose selectivity (67.00%). Further increasing $CaCl_2$ to 0.4 M and decreasing CaO to 0.1 M led to a significant drop in conversion (31.84%) and moderate selectivity (43.90%). In contrast, a control experiment using 0.5 M $CaCl_2$ without CaO yielded minimal conversion (14.47%) and tagatose selectivity (8.34%). These results emphasize that Ca^{2+} alone is insufficient for effective galactose isomerization.

We then conducted galactose (0.5 M) isomerization with various molar-ratio combinations of CaO and triethylamine[77] or arginine[39] (commonly used organic base catalysts) to further investigate the role of OH^- (**Figure 2-2c**). When reactions included higher CaO content (0.4 M CaO + 0.1 M arginine or triethylamine), we observed significantly higher galactose conversion (75.12% and 72.31%, respectively). In contrast, reactions with lower CaO and higher organic base (0.4 M triethylamine or arginine + 0.1 M CaO) showed much lower conversions (≤ 32.88%). Tagatose selectivity remained relatively constant across all cases (47.22–52.40%). These results highlight that CaO-derived OH^- ions are essential for maintaining the alkaline environment required for effective isomerization, whereas organic bases alone likely cannot sustain sufficient alkalinity.

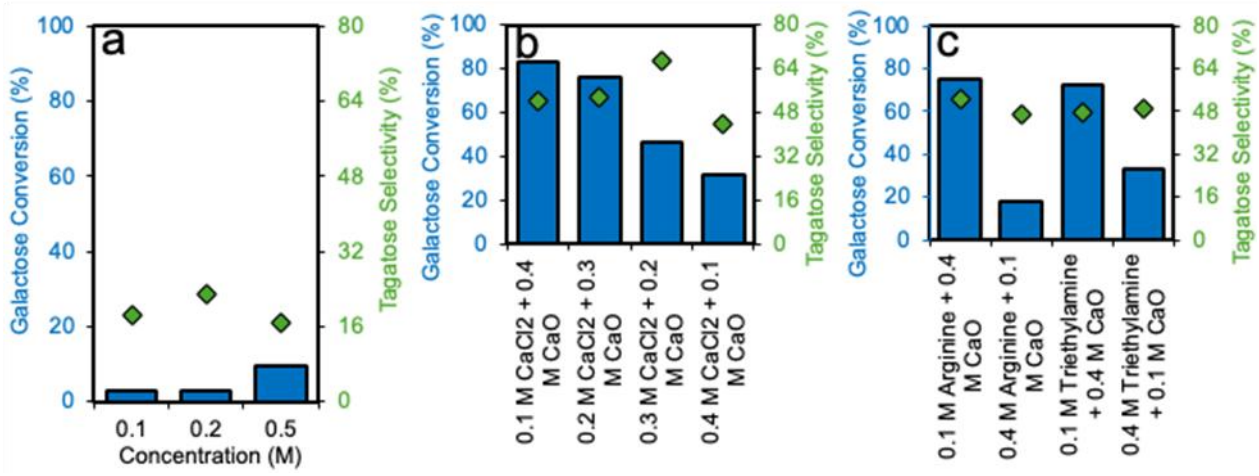

Figure 2-2. Galactose isomerization performance for (a) MgO, (b) CaO–$CaCl_2$, and (c) CaO–organic base systems (0.5 M galactose, 30 min reaction, CO_2 neutralization).

2.3.3 The mechanism of galactose isomerization to tagatose with CaO

Figure 2-3 shows a proposed scheme for galactose isomerization into tagatose with CaO in an aqueous solution. The OH^- derived from $Ca(OH)_2$ may initiate the isomerization by abstracting a proton from the α-carbon of galactose, forming a transient enediol intermediate.[28,78,79] In contrast, Ca^{2+} could coordinate with the cis-diol groups on galactose, particularly at the C1 and C2 positions, stabilizing the enediol intermediate and facilitating the rearrangement to tagatose, an entropy-favorable configuration. Water molecules might play a pivotal supporting role by participating in hydrogen bonding and proton shuttling,[75] which assist in stabilizing transition states and facilitating proton transfers throughout the reaction. Why did CaO exhibit significantly superior galactose isomerization performance compared to MgO? When CaO or MgO is added to a galactose solution, it reacts with water to yield $Ca(OH)_2$ or $Mg(OH)_2$, respectively. Firstly, $Mg(OH)_2$ exhibits lower water solubility than $Ca(OH)_2$. The latter, having a greater concentration of OH^-, would deprotonate more galactose to form an enediol intermediate. Secondly, compared to Ca^{2+}, Mg^{2+} may be incapable of stabilizing the enediol intermediate through coordination. It could be attributed to the fact that Ca^{2+} (ionic radius = 1.00 Å) possesses a stronger affinity for sugar hydroxyl groups, enabling crosslinked gel networks, whereas Mg^{2+} (ionic radius = 0.72 Å) exhibits weaker coordination capabilities.51–55 Here, we can conclude that OH^- and Ca^{2+} from CaO play a crucial role in deprotonating galactose and coordinating the sugar, respectively. Consequently, it might be impossible to effectively promote the isomerization of galactose without either OH^- or Ca^{2+}.

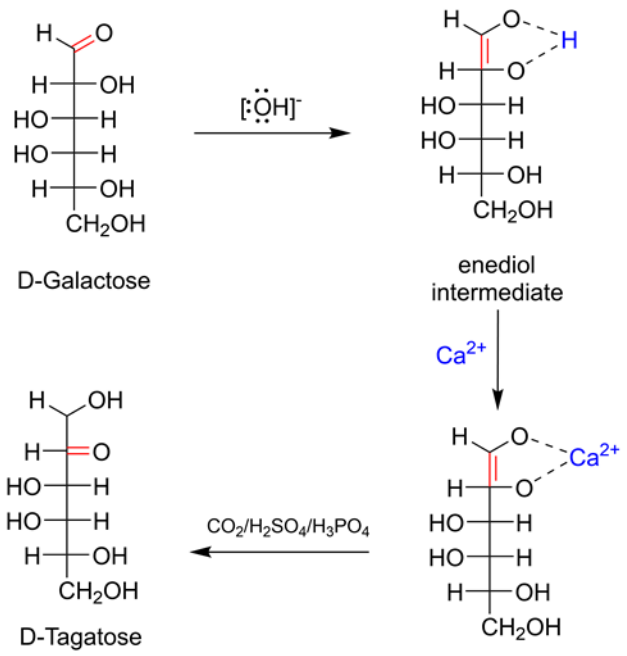

Figure 2-3. The proposed mechanism of galactose isomerization to tagatose with CaO.

2.3.4 Techno-economic analysis and sensitivity analysis

Figure 2-4a shows the galactose conversion and tagatose selectivity at a CaO/galactose molar ratio of 1/1 in a 0.5 M galactose solution, followed by the neutralization with H_3PO_4, H_2SO_4, or CO_2. It was found that H_3PO_4 resulted in a higher galactose conversion (89.10% vs. 69.11% and 86.65%) but a lower tagatose selectivity (53.59% vs. 73.20%) compared to neutralizing with H_2SO_4 and higher (53.59% vs. 50.47%) compared to neutralizing with CO_2 (**Figure 2-4a**). Overall, the highest tagatose yield of 50.59% was obtained through H_2SO_4 neutralization, followed by H_3PO_4 (47.75%) and CO_2 (43.73%). We performed TEA to obtain the MSP of tagatose with a detailed cost breakdown of producing 1 kg of 99% tagatose, incorporating both CAPEX and OPEX for the three neutralization (CO_2, H_2SO_4, or H_3PO_4) scenarios. The lowest MSP of tagatose was achieved with H_2SO_4 neutralization at \$0.80/kg, followed by CO_2 at \$0.81/kg and H_3PO_4 at \$0.85/kg (**Figure 2-4b**). This indicates that tagatose produced with this technology will be more

affordable than allulose ($19.8-$48.5/kg).[80] In the detailed cost breakdown, the contribution of OPEX to the MSP of tagatose accounts for $0.77-$0.83/kg across the three scenarios, while the CAPEX contributes only $0.02-$0.03/kg (**Figure 2-4b**). Moreover, the primary category contributing to the differences in the MSP of tagatose among the three neutralization methods was the costs associated with the facility.

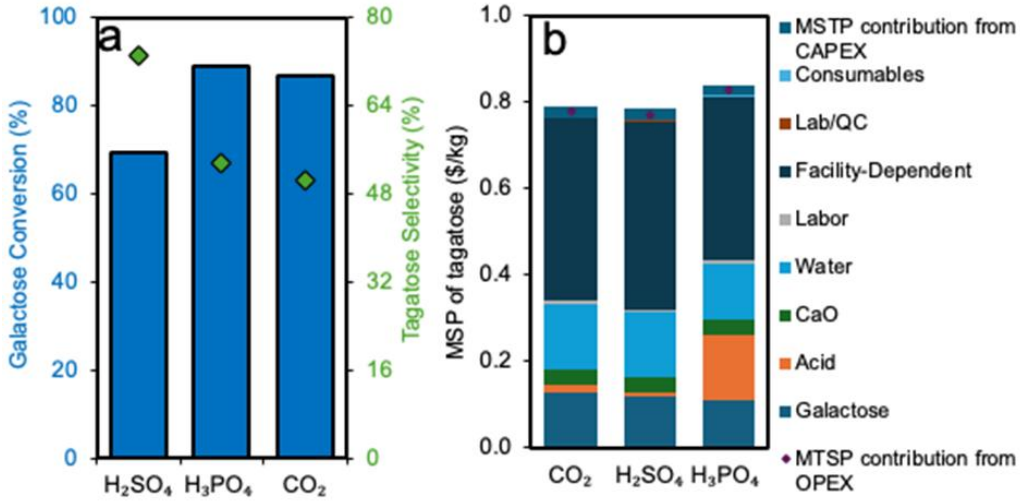

Figure 2-4. Isomerization of galactose to tagatose with CaO followed by H_2SO_4 or H_3PO_4 or CO_2 neutralization in a 0.5 M galactose solution with a CaO/galactose molar ratio of 1/1. (b) MSP of tagatose per kg in three scenarios with detailed CAPEX and OPEX contribution.

A sensitivity analysis was performed to identify the key drivers influencing the MSP of tagatose for the CO_2 neutralization scenario (**Figure 2-5**). Plant capacity and IRR are the most impactful factors on the MSP of tagatose. For instance, increasing the plant capacity from 50 MT/day to 150 MT/day raises the MSP of 1 kg tagatose from $0.78/kg to $0.85/kg, while an increase in the IRR from 5% to 15% leads to a notable rise in the MSP of tagatose from $0.76/kg to $0.84/kg. The third major sensitive factor is galactose cost. Changing the price of galactose from $218/MT to $653/MT results in an increase in the MSP of tagatose from $0.78/kg to $0.83/kg. CaO cost and CAPEX have similar impacts on the MSP of 1 kg tagatose. Increasing the

CAPEX from $27M to $81M and the CaO cost from $100/MT to $300/MT changes the MSP from $0.79/kg to $0.82/kg.

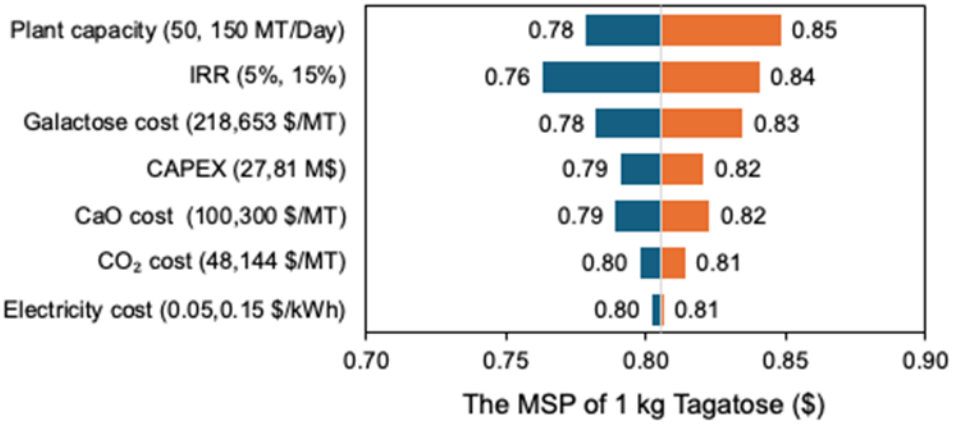

Figure 2-5. Sensitivity analysis of MSP of 1 kg tagatose for the CO_2 neutralization scenario with a 50% decrease or increase in the baseline of plant capacity (100 MT/Day), IRR (10%), CAPEX (54 M$), galactose cost ($435.00/MT), CaO cost ($200.00/MT), CO_2 cost ($96), and electricity cost ($0.10/kWh).

2.3.5 Global warming potential and life-cycle impact assessment

The CO_2 neutralization scenario had the lowest GWP at 0.90 CO_2eq/kg tagatose, compared to 2.54 CO_2eq/kg tagatose for H_2SO_4 and 2.69 CO_2eq/kg tagatose for H_3PO_4 (Fig. 6a). This difference arose primarily from the acid contribution, where CO_2 neutralization provides a -1.19 CO_2eq/kg tagatose credit, due to CO_2 sequestration during the formation of insoluble $CaCO_3$. In contrast, H_2SO_4 and H_3PO_4 contributed positively to GWP at 0.31 and 0.44 CO_2eq/kg tagatose, respectively, reflecting the environmental burden of acid production and disposal. Other contributors such as transportation (0.05 CO_2eq/kg), CaO production (1.42 CO_2eq/kg), electricity (0.06 CO_2eq/kg), steam (0.49–0.64 CO_2eq/kg), and water (0.07–0.08 CO_2eq/kg) remained relatively consistent across scenarios. These findings highlight that using CO_2 to neutralize the gel complex not only facilitates a practical quenching method for the isomerization reaction but also offers a more sustainable approach for tagatose production by minimizing the carbon footprint.

Fig. 6b displays the normalized life-cycle environmental impacts for 1 kg of tagatose. Among the three scenarios, H_2SO_4 neutralization exhibited the highest environmental impacts in nearly all categories (Fig. 6b), except for GWP (90.65%), EU (89.91%), and FFD (89.59%). H3PO4 neutralization showed the highest impact for the three categories (GWP, EU, and FFD). It is clear that CO_2 neutralization exhibited the lowest environmental impacts, with only 19.91% in GWP and 67.54-78.01% in other categories (**Figure 2-6b**).

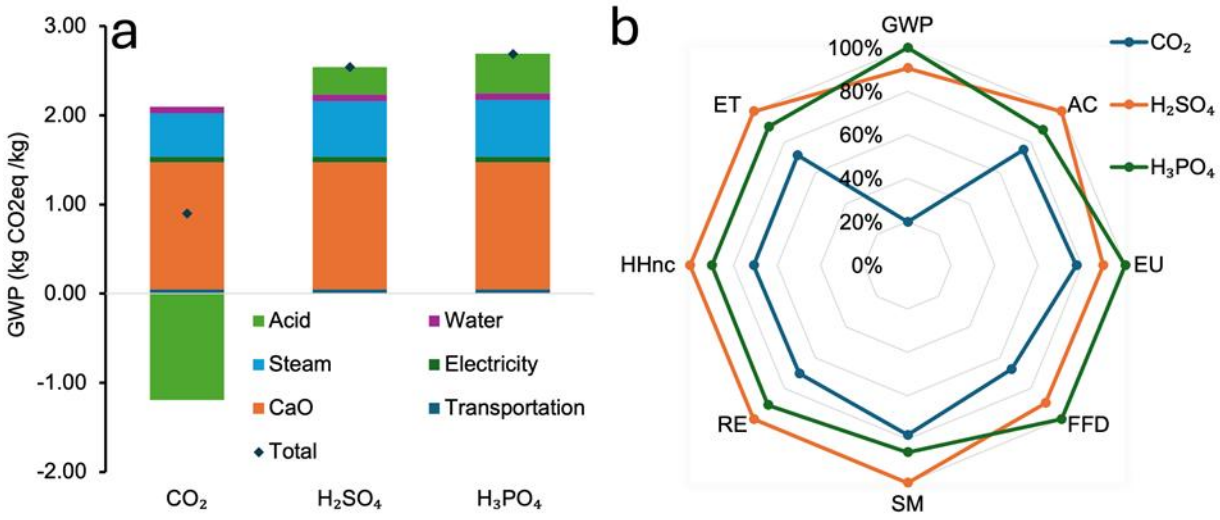

Figure 2-6. Life-cycle GWP (a) and LCIA (b) of 1 kg tagatose for the three scenarios. The value (%) of each environment impact category was calculated based on the highest one (100%) among the scenarios.

2.4. Conclusion

This study presents a green and economically viable reaction process for rare sugar manufacturing, specifically tagatose production from galactose, through CaO-promoted isomerization followed by CO_2 neutralization under ambient conditions. Isomerization with a CaO/galactose molar ratio of 1/1 in a 0.5 M galactose solution, followed by CO_2 neutralization, resulted in a galactose conversion of 86.65% and a tagatose selectivity of 50.47%, namely, a tagatose yield of 43.73%. By increasing the CaO/galactose molar ratio and galactose

concentration, galactose conversion was significantly enhanced. However, replacing CaO with MgO, $CaCl_2$, triethylamine, or arginine led to a substantial decrease in galactose conversion. The OH^- and Ca^{2+}, derived from CaO, played distinct yet crucial roles in the isomerization of galactose to tagatose. Among the neutralization scenarios involving CO_2, H_2SO_4, or H_3PO_4, CO_2 neutralization achieved a comparable MSP of tagatose (0.81/kg) with the lowest environmental impacts. These findings provide critical insights into the development of scalable, eco-friendly, and nonenzymatic sugar isomerization processes.

Chapter 3 - Kinetics and Thermodynamic Analysis of Galactose Isomerization to Tagatose

Portions of this chapter have been published previously in the following article: Babaei, S. et al. “Catalytic Kinetic and Thermodynamics of Galactose Isomerization to Tagatose With a Homogeneous Triethylamine Catalyst,” ChemCatChem, 2026, 18, e01681, Doi.org/10.1002/cctc.202501681. The author of this thesis was the first author of the publication and was primarily responsible for experimental design, data analysis, and manuscript preparation.

3.1. Introduction

Global overconsumption of caloric sweeteners has contributed to a sharp rise in metabolic disorders.[81] In 2023, global sugar consumption exceeded 187.4 million metric tons, while 38% of adults were overweight and 13% were obese, with diabetes cases tripling since 1980 to 536.6 million and projected to reach 783.2 million by 2045.[82–85] These trends have intensified the demand for low-calorie sugar alternatives with comparable sweetness to sucrose.[14] Among emerging rare sugars, tagatose delivers 90% of sucrose sweetness but only 1.5 kcal g^{-1} (compared to 3.9 kcal g^{-1} for sucrose), possesses a glycemic index of 3 (sucrose = 65), and exhibits prebiotic and antihyperglycemic activity.[58,86] As a generally recognized as safe (GRAS) certified compound, tagatose is increasingly utilized in beverages, confectionery, and dairy formulations.[87] However, the high production cost, stemming from slow enzymatic conversion of galactose to tagatose and low equilibrium yields, remains the principal barrier to commercialization.[28] Developing efficient catalytic pathways for galactose-to-tagatose isomerization, the key step in tagatose synthesis, is therefore essential for sustainable and scalable rare-sugar production.[88,89]

The conversion of D-galactose to D-tagatose has historically relied on L-arabinose isomerase obtained from various microbial sources such as Lactobacillus plantarum and Escherichia coli.[16,90,91] Although these enzymes catalyze the reaction efficiently in water, they typically reach less than 60% conversion within one to three days and exhibit limited heat stability beyond 60 °C due to dependence on metal cofactors like Co^{2+}or Mg^{2+}. These drawbacks restrict their large-scale use and have stimulated exploration of alternative, non-enzymatic catalytic systems.[92–95] In recent years, heterogeneous bases (e.g., CaO, MgO),[23,35,75] hydrotalcite,[22,71] and Lewis acid zeolites (e.g., Sn-β)[31,96,97] have demonstrated activity for sugar isomerization, while organic Brønsted bases such as triethylamine (Et_3N) and arginine,[32,39,98,99] offer a metal-free, homogeneous route.[78,100] Et_3N, in particular, facilitates reversible C-2 epimerization of aldoses through an enediol intermediate consistent with the Lobry de Bruyn–van Ekenstein (LdBE) mechanism.[33,79,101] In glucose–fructose systems, Et_3N exhibits first-order kinetics with an apparent activation energy of 61 kJ/mol,[102] and in the galactose to tagatose isomerization, it achieves up to 52% galactose conversion and 40.8% tagatose selectivity at 100 °C after 40 min, although the selectivity declines over time as a result of tagatose degradation and humin formation.[75] While strongly basic conditions are widely recognized as unfavorable for glucose–fructose isomerization due to rapid alkaline degradation, multiple studies have demonstrated that galactose–tagatose interconversion can proceed effectively under basic environments.[103] This distinction reflects fundamental differences in sugar chemistry and supports the use of homogeneous base catalysis as a meaningful framework for probing galactose isomerization kinetics, rather than as a direct process optimization strategy.

Despite these advances, no detailed kinetic or thermodynamic framework currently exists to describe the reversible galactose to tagatose to talose transformations and concurrent byproduct

formation under homogeneous base catalysis, leaving the reaction mechanism and rate-determining steps insufficiently quantified. The interplay between kinetic control at short reaction times and thermodynamic control at equilibrium remains unresolved. Furthermore, while byproduct formation is recognized as a major cause of declining tagatose selectivity, its quantitative relationship with the isomerization kinetics has never been modeled.[104] To address these gaps, the present study develops a mechanistic kinetic framework that integrates experimental measurements and theoretical analysis to capture the reversible isomerization and irreversible degradation pathways of galactose in aqueous triethylamine solutions across a wide temperature range.

The kinetic and thermodynamic insights obtained from this study provide the first quantitative framework for describing the base-catalyzed isomerization of galactose to tagatose under homogeneous conditions. By integrating reversible and irreversible pathways within a thermodynamically consistent model, this work bridges the gap between empirical observations of sugar conversion and the underlying reaction mechanisms. The extracted parameters: rate constants, equilibrium constants, and activation energies, offer a predictive basis for optimizing reaction conditions to maximize tagatose yield while minimizing degradation. Beyond galactose chemistry, the approach established here can be extended to other aldose–ketose transformations, contributing to a more fundamental understanding of enediol-mediated isomerization kinetics in carbohydrate systems.

3.2. Experimental Section

3.2.1 Tagatose synthesis

Galactose (purity ≥ 99%), tagatose (purity ≥98%), talose (purity ≥ 99%), and Et_3N (liquid, ≥ 99.5%) were purchased from Sigma-Aldrich (St. Louis, MO). The Et_3N (15 mol% relative to

galactose) was introduced into a Teflon-lined reactor containing 9 mL of a galactose (0.52 M) solution. The reactor was equipped with a magnetic stirrer operating at 500 rpm for the 1 to 20 min at temperatures ranging from 40 °C to 100 °C with a sealed Teflon-lined reactor immersed in an oil bath. Following that, the resulting solution was transferred to an ice bath to quench the reaction and then moved to a carbonation machine (SodaStream International Ltd., United Kingdom) to neutralize residual Et_3N with CO_2 and stabilize tagatose by forming bicarbonate buffer. Carbonation with CO_2 was employed exclusively as a rapid quenching step to neutralize triethylamine and immediately quench base-catalyzed isomerization.[102] Upon CO_2 addition, triethylamine is rapidly protonated according to Eq. (1), resulting in a near-neutral pH, a regime in which aldose–ketose interconversion via the LdBE mechanism is kinetically negligible, since enediol intermediates are only transiently stabilized under alkaline conditions, rapid protonation effectively collapses these species and preserves the relative sugar distributions at the quench time.[100,105] The transient increase in ionic strength associated with bicarbonate formation during CO_2 carbonation is not expected to affect the equilibria of neutral sugar species on the experimental timescale.[79] The pH of the resulting solution, typically ranged from 6 to 7 corresponds to the post-reaction quenching stage after CO_2 carbonation and does not reflect the reaction pH during the isomerization step. The precipitate was filtered out using a 0.22 μm VMR brand membrane. No measurable loss of tagatose was observed during the quenching or subsequent filtration steps within the resolution of the HPLC analysis.[23] Liquid samples were diluted fivefold with HPLC-grade water prior to compositional analysis. Galactose and tagatose concentrations were determined using an Agilent 1200 HPLC system, which was equipped with a Refractive Index Detector and a Rezex RCM-Monosaccharide column (Phenomenex, Torrance,

CA). The HPLC-grade water served as the mobile phase at a flow rate of 0.6 mL/min, while the column temperature was maintained at 80 °C.[23]

$$^{-}_{3}Et_3N + CO_2 + H_2O \rightarrow Et_3NH^+ + HCO \quad (1)$$

3.2.2 Kinetic calculations

The Et_3N-catalyzed isomerization of galactose (G) to tagatose (T) and talose (L) was modeled as a reversible three-component network accompanied by irreversible degradation (**Figure 3-1**). Consistent with an enediol mechanism, each elementary step was assumed first order in sugar and first order in base.[79] Since the total Et_3N concentration remained constant under the reaction conditions, the overall kinetics were treated as pseudo–first-order with respect to sugar. The elementary rate laws are therefore as Eqs. (2)-(4):

$$r_{ij}^{f} = C_E k_{ij}^{f} C_i \quad (2)$$

$$r_{ij}^{r} = C_E k_{ij}^{r} C_i \quad (3)$$

$$r_{i\rightarrow B} = C_E k_{i\rightarrow B} k_i^{r} C_i \quad (4)$$

Where C_i is sugar concentration, which C_G, C_T, C_L, and C_B (mM) represent the concentrations of galactose, tagatose, talose, and the lumped byproduct, respectively. C_E (mM) is the total Et_3N concentration. Each reversible isomerization step is characterized by a forward and reverse rate constant, k_{ij}^{f} and k_{ij}^{r} (min^{-1}), while the irreversible degradation of each sugar is represented by the first-order constants $k_{i\rightarrow B}$ of the same unit.

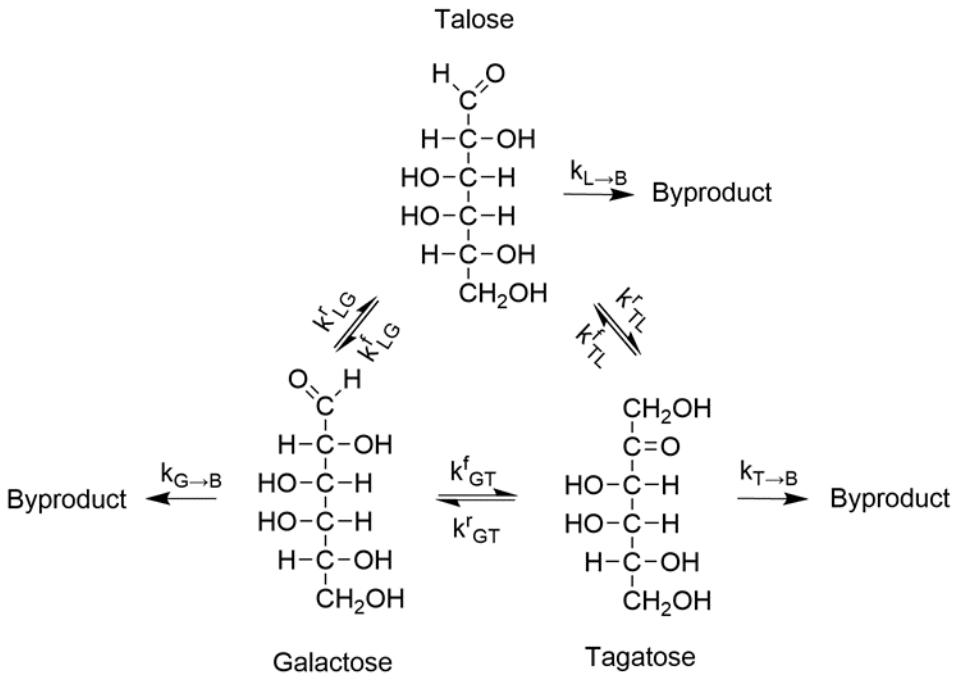

Figure 3-1. Proposed kinetic and thermodynamic network for the Et_3N-catalyzed isomerization of galactose (G) to tagatose (T) and talose (L).

Accordingly, the reaction network consists of the reversible conversions between galactose and tagatose, and between tagatose and talose, while talose can reversibly interconvert with galactose to ensure thermodynamic closure of the cycle. Parallel to these reversible steps, each sugar may undergo irreversible degradation to a lumped byproduct pool, representing the formation of humins and other side-products observed at elevated temperatures. Under these assumptions, the temporal evolution of each species was described by the following set of differential rates as Eqs. (5)-(8) and solved in Python using SciPy (solve_ivp, LSODA).

$$\frac{dC_G}{dt} = C_E[-k_{GT}^f C_G + k_{GT}^r C_T - k_{LG}^r C_G + k_{LG}^f C_L - k_{G\to B} C_G] \quad (5)$$

$$\frac{dC_T}{dt} = C_E[+k_{GT}^f C_G - k_{GT}^r C_T - k_{TL}^f C_T + k_{TL}^r C_L - k_{T\to B} C_T] \quad (6)$$

$$\frac{dC_L}{dt} = C_E[+k_{TL}^f C_T - k_{TL}^r C_L - k_{LG}^f C_L + k_{LG}^r C_G - k_{L\to B} C_L] \quad (7)$$

$$\frac{dC_B}{dt} = C_E[k_{G\to B}C_G + k_{T\to B}C_T + k_{L\to B}C_L] \quad (8)$$

The equilibrium constants of the reversible reactions are defined as Eqs. (9)-(11):

$$K_{GT} = \frac{k_{GT}^f}{k_{GT}^r} \quad (9)$$

$$K_{TL} = \frac{k_{TL}^f}{k_{TL}^r} \quad (10)$$

$$K_{LG} = \frac{k_{LG}^f}{k_{LG}^r} \quad (11)$$

and satisfy the thermodynamic closure condition ensuring detailed balance within the isomerization cycle (Eq. (12):

$$K_{GT} \times K_{TL} \times K_{LG} = 1 \quad (12)$$

3.2.3 Thermodynamic calculations

The temperature dependence of the kinetic and equilibrium parameters was evaluated to obtain the activation and thermodynamic quantities for each isomerization/epimerization step. Apparent rate constants obtained at different temperatures were correlated using the Arrhenius and Eyring equations, while equilibrium constants were analyzed through the van't Hoff relation. These correlations provided the activation energy (E_a), activation enthalpy ($\Delta H^{\ddagger}$), and activation entropy ($\Delta S^{\ddagger}$), for the forward isomerization reactions, as well as the standard reaction enthalpy (ΔH°), standard entropy (ΔS°), and Gibbs free-energy change (ΔG°).

The temperature dependence of each apparent rate constant $k_{ij}^f$was first represented by Eq. (13):

$$k_{ij}^f = A_{ij} exp\left(-\frac{E_{a,ij}}{RT}\right) \quad (13)$$

Where A_{ij} is the pre-exponential factor, $E_{a,ij}$ (kJ mol^{-1}) is the apparent energy, R is the gas constant (8.314J mol^{-1} K^{-1}), and T is the absolute temperature (K). A linear plot of ln k_{ij}^{f} versus 1/T yields the slope -$E_{a,ij}$/R and intercept ln A_{ij}.

To separate the enthalpic and entropic contributions to the activation barrier, the rate constants were also expressed using the Eyring equation (Eq. (14):

$$ln\left(\frac{k_{ij}^{f}}{T}\right) = -\frac{-\Delta H_{ij}^{\ddagger}}{R}\frac{1}{T} + ln\left(\frac{k_B}{h}\right) + \frac{\Delta S_{ij}^{\ddagger}}{R} \quad (14)$$

Where k_B and h are the Boltzmann and Planck constants, respectively, $\Delta H_{ij}^{\ddagger}$ (kJ mol^{-1}) is the activation enthalpy, and $\Delta S_{ij}^{\ddagger}$ (J mol-1K^{-1}) is the activation entropy. The slope of ln (k/T) versus 1/T provides $\Delta H_{ij}^{\ddagger}$/R, and the intercept yields ln $\left(\frac{k_b}{h}\right) + \Delta S^{\ddagger}/R$.

The equilibrium constants K_{ij} for the reversible isomerization steps were correlated by the van't Hoff equation (Eq. (15):

$$lnK_{ij} = -\frac{-\Delta H_{ij}^{\circ}}{R}\frac{1}{T} + \frac{\Delta S_{ij}^{\circ}}{R} \quad (15)$$

Where ΔH_{ij}° (kJ mol^{-1}) and ΔS_{ij}° (J mol^{-1}K^{-1}) represent the standard enthalpy and entropy change of reaction, respectively. From these values, the standard Gibbs free-energy change at any temperature can be determined as Eq. (16):

$$\Delta G_{ij}^{\circ} = \Delta H_{ij}^{\circ} - T\Delta S_{ij}^{\circ} = -RTlnK_{ij} \quad (16)$$

All thermodynamic quantities were calculated using the parameters derived from the kinetic modeling at four temperatures (40-100 °C). The resulting $\Delta H_{ij}^{\ddagger}$,$\Delta S_{ij}^{\ddagger}$,ΔH_{ij}°,ΔS_{ij}°, and ΔG_{ij}° values were used later to interpret the temperature effects on the reaction equilibria and catalytic performance.

3.2.4 Validation and error analysis

Each experiment was repeated at least twice (n=2) per time point for each temperature to ensure reproducibility, while reported concentrations are mean values and the replicate-to-replicate variability was within ±5%. Given the small experimental variability relative to the concentration scale, error bars were omitted from the time-course plots for clarity. The thermodynamic consistency of equilibrium constants was verified through Eq. (17):

$$K_{GT} \times K_{TL} \times K_{LG} = 1 \quad (17)$$

Kinetic parameters (θ) were obtained by minimizing a nonlinear least-squares objective function as Eq. (18). Parameter uncertainties are reported as one-standard-deviation estimates (±1σ) derived from the Jacobian-based covariance matrix as Eq. (19),

$$\Phi(\boldsymbol{\theta}) = \sum_{i=1}^{N_t} \sum_{j=1}^{N_s} (C_{j,i}^{model}(\theta) - C_{j,i}^{exp})^2 \quad (18)$$

$$Cov(\theta) \approx s^2 (J^T J)^{-1}, \; s^2 = \frac{SSR}{m-n} \quad (19)$$

In Eq. (18), Φ(θ) denotes the objective function, , $C_{j,i}^{\text{model}}(\boldsymbol{\theta})$ and $C_{j,i}^{\text{exp}}$ are the model-predicted and experimentally measured concentrations of species j at time point i, respectively, N_s is the number of chemical species, and N_t is the number of sampling time points. In Eq. (19), J is the Jacobian matrix of partial derivatives of the residuals with respect to the fitted parameters, m is the total number of residuals, n is the number of fitted parameters, and s^2 represents the estimated residual variance.

3.3. Results and Discussion

At 40 °C, the reaction proceeded slowly, reaching only 30 % galactose conversion and 57% selectivity after 300 min, respectively (Fig. 2A). the low (k_{GT}^{f}=2.44 × 10^{-5} min^{-1}) and equilibrium constant (K_{GT}=0.6) indicate that both kinetics and thermodynamics restrict conversion at this

temperature (**Table 2**). Raising the temperature to 60 °C increased k_{GT}^{f} by 8% to 2.63×10^{-5} min^{-1} and K_{GT}=0.8 enabling faster equilibration for galactose to tagatose and higher galactose conversion up to 41% but slightly lower tagatose selectivity to 36% due to mild byproduct formation. The minor rise in (k_{TL}^{f}=2.57×10^{-5} min^{-1}) and K_{TL}=0.09 explains the small but noticeable increase in talose. However, the first signs of degradation appear, as shown by the modest rise in ($k_{G \to B}$=3.79×10^{-5} min^{-1}), consistent with the slight increase in byproduct concentration (**Fig. 3-2B**).

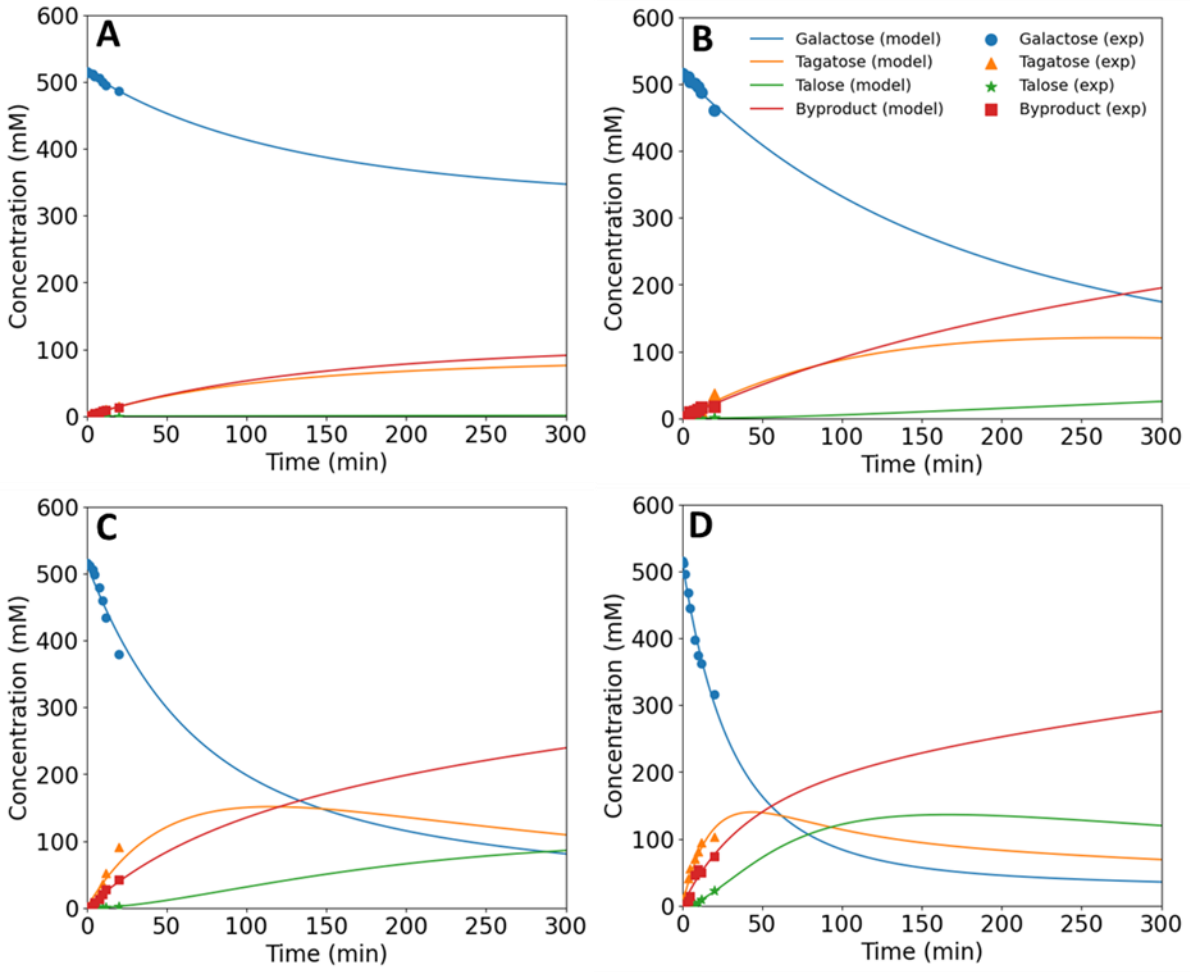

Figure 3-2. Experimental and simulated concentration–time profiles for Et_3N-catalyzed galactose isomerization to tagatose and talose at (A) 40 °C, (B) 60 °C, (C) 80 °C, and (D) 100 °C. Symbols represent experimental data and solid lines denote model predictions.

At 80 °C, equilibrium of galactose to tagatose was established within 100 min, consistent with a nearly tenfold rise in k_{GT}^{f}=1.7 × 10^{-4} min^{-1} and a further increase in K_{GT}=0.87 yielding almost 65% galactose conversion and 47% selectivity, while the talose-forming path became more competitive (k_{TL}^{f}=2.57 × 10^{-5} min^{-1}), doubling the talose concentration relative to 60 °C (**Figure 3-2C**). The larger equilibrium constant reflects a thermodynamic shift that slightly favors tagatose formation, although the irreversible loss constants ($k_{G\rightarrow B}$=6.93 × 10^{-5} min^{-1}) begin to compete.

Further heating to 100 °C accelerated the reaction dramatically; Over the first 50 min, corresponding to 70% galactose conversion, but selectivity decreased to 38% due to rapid degradation (**Figure 3-2D**). At this temperature, the k_{GT}^{f} rose to 4.58× 10^{-4} min^{-1}, nearly 19 times higher than at 40 °C, while K_{GT}=0.99 approached unity, indicating near-thermodynamic equilibrium between galactose and tagatose. The concurrent rise in irreversible rate constants ($k_{G\to B} = 2.02 \times 10^{-5}$ min^{-1}, $k_{T\to B}$=1.23 × 10^{-19} min^{-1}, $k_{L\to B}$=2.15 × 10^{-20} min^{-1}) explains the extensive byproduct accumulation. At this temperature, the talose pathway remained kinetically viable (k_{TL}^{f}=3.85 × 10^{-4} min^{-1}), but the equilibrium K_{TL}=0.25 still favored tagatose.

Table 2. Fitted kinetic and equilibrium parameters for the triethylamine-catalyzed isomerization of galactose to tagatose and talose at different temperatures (40–100 °C).

k_{GT}^{f}	k_{GT}^{r}	K_{GT}	k_{TL}^{f}	k_{TL}^{r}	K_{TL}	k_{LG}^{f}	k_{LG}^{r}	K_{LG}	$k_{G\to B}$	$k_{T\to B}$	$k_{L\to B}$	R_G^2	R_T^2	R_L^2	R_B^2
						40									
2.44	4.08		2.32	6.26		6.24	1.57		2.78	7.35	3.16				
× **10^{-5}**	× 10^{-}	.60	× 10^{-6}	× 10^{-}	.04	× 10^{-4}	× 10^{-4}	9.75	× 10^{-}	× 10^{-2}	× 10^{-30}				
± **4.30**	± 7.7	5.09 ×	± 4.70	± 2.5(	±2.6	± 6.09	± 2.12	±1.65	± 4.6	± 5.1	± 2.61	.97	.93	.91	.9
× **10^{-7}**	× 10^{-}	10^{-2}	× 10^{-7}	× 10^{-}	10^{-2}	× 10^{-4}	× 10^{-4}		× 10^{-}	× 10^{-2}	× 10^{-31}				6
						60									
2.63	3.30		2.57	2.91		7.30	5.14		3.79	1.79	6.95				
× **10^{-5}**	× 10^{-}	.80	× 10^{-5}	× 10^{-}	.09	× 10^{-4}	× 10^{-4}	4.20	× 10^{-}	× 10^{-2}	× 10^{-29}				
± **1.16**	± 1.6	±1.61	± 5.79	± 5.8(	±3.44	± 5.78	± 4.69	±4.30	± 6.5	± 3.1	± 5.91	.95	.89	.93	.9
× **10^{-6}**	× 10^{-}	10^{-2}	× 10^{-6}	× 10^{-}	× 10^{-}	× 10^{-4}	× 10^{-4}	0.48	× 10^{-}	× 10^{-2}	× 10^{-30}				0

80													
1.70	1.95	(	5.47	2.74	2.10	4.08		6.93	5.11	2.56			
$\times$ **10^{-4}**	$\times 10^{-}$	.87	$\times 10^{-5}$	$\times 10^{-}$	.2	$\times 10^{-4}$	$\times 10^{-4}$	.14	$\times 10^{-}$	$\times 10^{-2}$	$\times 10^{-27}$			
$\pm$ **1.03**	$\pm$ 9.7	$\pm$5.59	$\pm$ 5.52	$\pm$ 5.2	$\pm$1.04	$\pm$ 6.97	$\pm$ 1.03	$\pm$6.42	$\pm$ 2.67	$\pm$ 7.05	$\pm$ 3.65	.91	.87	.92	.95
$\times$ **10^{-5}**	$\times 10^{-}$	10^{-2}	$\times 10^{-6}$	$\times 10^{-}$	$\times 10^{-}$	$\times 10^{-4}$	$\times 10^{-4}$	10^{-1}	$\times 10^{-}$	$\times 10^{-2}$	$\times 10^{-28}$				
100													
4.58	4.60	(	3.85	1.57	4.34	1.05		2.02	1.23	2.15			
$\times$ **10^{-4}**	$\times 10^{-}$	.99	$\times 10^{-4}$	$\times 10^{-}$	.25	$\times 10^{-3}$	$\times 10^{-3}$	.13	$\times 10^{-}$	$\times 10^{-1}$	$\times 10^{-20}$				
$\pm$ **1.27**	$\pm$ 1.0	$\pm$3.97	$\pm$ 1.49	$\pm$ 1.2	$\pm$7.48	$\pm$ 3.79	$\pm$ 8.00	$\pm$2.70	$\pm$ 3.4	$\pm$ 5.06	$\pm$ 1.61	.98	.96	.96	.92
$\times$ **10^{-5}**	$\times 10^{-}$	10^{-2}	$\times 10^{-5}$	$\times 10^{-}$	$\times 10^{-}$	$\times 10^{-3}$	$\times 10^{-3}$	10^{-2}	$\times 10^{-}$	$\times 10^{-2}$	$\times 10^{-21}$				

Overall, the temperature dependence of all kinetic parameters follows the expected Arrhenius behavior, whereas the equilibrium constants (K_{GT} and K_{TL}) increase slightly with temperature, confirming an endothermic reaction process. The continuous rise in the irreversible loss constants demonstrates that degradation pathways are far more temperature-sensitive than reversible isomerization. Consequently, the data delineates a clear operating window, moderate temperature (80 °C) and limited residence time (< 1 h), where galactose conversion and tagatose yield are maximized before byproduct formation becomes dominant.

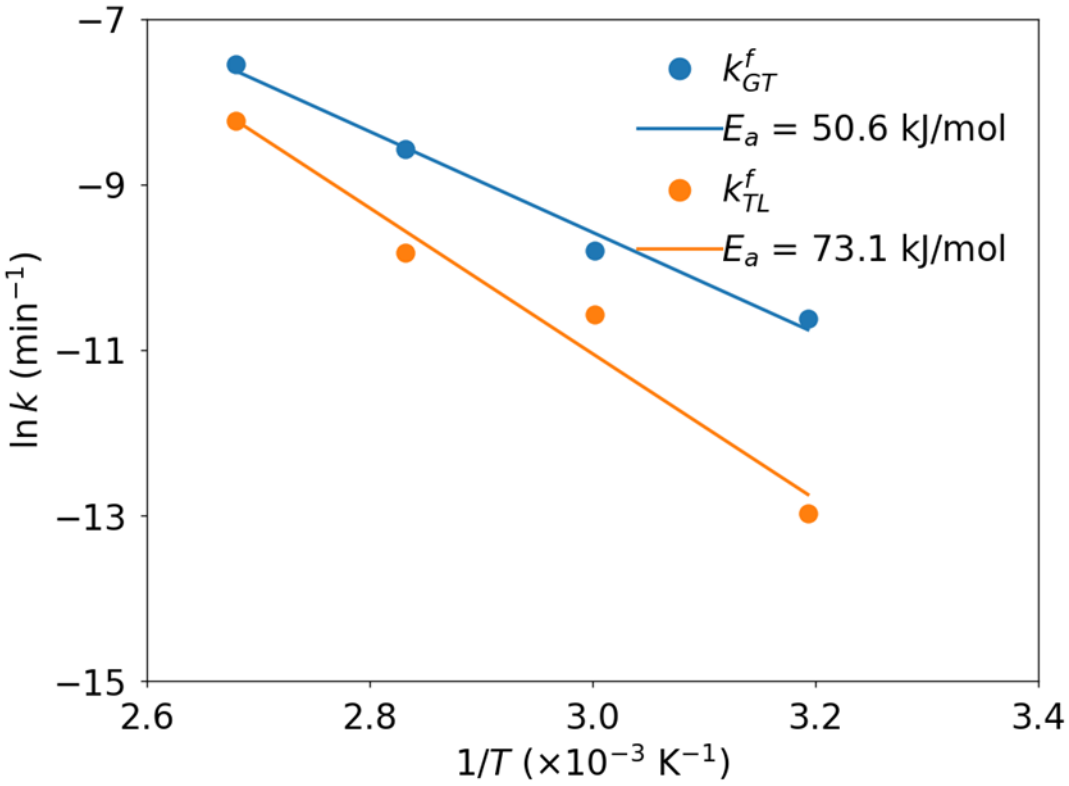

Figure 3-3. Arrhenius plots for the forward rate constants of the galactose to tagatose and tagatose to talose isomerization reactions. Apparent rate constants ($\boldsymbol{k^f_{GT}}$, $\boldsymbol{k^f_{TL}}$) were obtained from kinetic fitting at 40–100 °C with R^2 above 0.96.

Table 3. Summary of activation energies (E_a) for aldose–ketose isomerization reactions in various catalytic media.

Reaction	**Catalyst**	$\boldsymbol{E_a}$ **(kJ mol^{-1})**	**Ref**
Glucose to fructose	Amidoximed Polyacrylonitrile	79.7	[106]
Glucose to fructose	Sn-β	93	[107]
Glucose to fructose	$AlCl_3$	110	[108]
Glucose to fructose	NaOH	121	[109]
Glucose to fructose	$MgCl_2$-700	60	[110]

Glucose to fructose	$AlCl_3$,$6H_2O$	110	[111]
Glucose to fructose	$CrCl_3$.$6H_2O$	62.5	[102]
Glucose to fructose	$SnCl_4$.$5H_2O$	96.5	[102]
Glucose to fructose	Et_3N	61	[102]
Galactose to tagatose	Et_3N	50.6 ± 4	This study
Tagatose to talose	Et_3N	73.1 ± 9	This study

The E_a for the galactose to tagatose step (50.6 ± 4 kJ mol^{-1}) was lower than that for the tagatose to talose step (73.1 ± 9 kJ mol^{-1}), indicating that the epimerization pathway requires a higher energetic barrier than the isomerization (**Figure 3-3**). These values are consistent with previously reported base-catalyzed transformations of hexoses, where enediol formation constitutes the rate-determining step (**Table 3**). The relatively small E_a confirms that Et_3N effectively lowers the reaction barrier through reversible proton transfer and stabilization of the enediol intermediate. The stronger temperature sensitivity of the tagatose to talose reaction suggests that this step is less catalytically favored and more thermally driven.[112] Overall, the Arrhenius analysis demonstrates that increasing temperature enhances both reaction rate and equilibrium conversion without altering the catalytic mechanism.

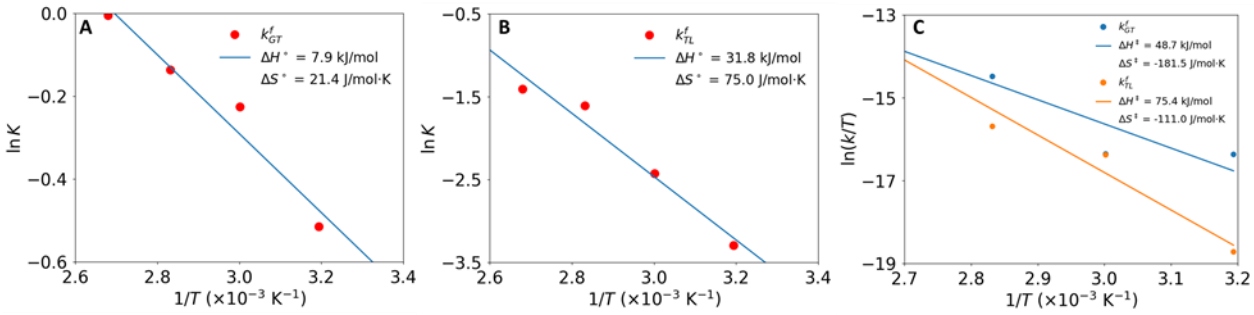

Figure 3-4. Van't Hoff plots for the forward isomerization steps, (A) for galactose to tagatose and (B) tagatose to talose equilibria; (C) Eyring plots for the corresponding forward rate constants.

The thermodynamic parameters derived from the van't Hoff and Eyring plots (**Figure 3-4**) reveal a consistent energetic framework for the Et_3N-catalyzed galactose isomerization. **Figure 3-4A** and **Figure 3-4B** show linear correlations for both galactose to tagatose and tagatose to talose equilibria ($R^2 > 0.88$). The van't Hoff plot for the tagatose–talose equilibrium (**Figure 3-4B**) exhibits slightly greater scatter than that for galactose–tagatose (**Figure 3-4A**), reflecting higher in ΔH° and ΔS°, which arises from the lower equilibrium concentration of talose that amplifies quantification error and from the greater mechanistic complexity of the C-2 epimerization step. The standard enthalpy changes ΔH° = 7.9 kJ mol^{-1} for galactose to tagatose and 31.8 kJ mol^{-1} for tagatose to talose confirm the endothermic character of the reactions, while the positive entropy changes (ΔS°= 21 J mol^{-1} K^{-1} for galactose to tagatose and 75 J mol^{-1} K^{-1} for tagatose to talose) suggest that higher temperature favors ketose formation by increasing molecular disorder. The larger ΔH° and ΔS° for tagatose to talose reflect greater configurational rearrangement and weaker hydrogen bonding in talose relative to tagatose.[113] These values are consistent with base-catalyzed aldose–ketose systems, confirming that the Et_3N system follows the general thermodynamic pattern of an entropy-driven enediol isomerization (**Table 4**). The positive ΔS° values likely arise from partial disruption of the hydrogen-bond network between sugar hydroxyls and water molecules, which releases structured solvent during the rearrangement.[102]

Figure 3-4C shows the Eyring plots derived from the temperature-dependent rate constants, yielding activation enthalpies ($\Delta H^\ddagger$) of 48.7 kJ mol^{-1} for galactose to tagatose and 75.4 kJ mol^{-1} for tagatose to talose and activation entropies ($\Delta S^\ddagger$) of –181 J mol^{-1} K^{-1} for galactose to tagatose and –111 J mol^{-1} K^{-1} for tagatose to talose, respectively. The negative $\Delta S^\ddagger$ values indicate highly ordered transition states, characteristic of concerted proton-transfer mechanisms proceeding

through an enediolate intermediate stabilized by triethylamine.[37] Et_3N acts as a bifunctional base that abstracts a proton from C2–OH while donating one to the carbonyl oxygen, forming a transient hydrogen-bonded complex.[10] This ordered transition structure reduces enthalpic demand but restricts configurational freedom, explaining the large negative $\Delta S^{\ddagger}$.

Table 4. Comparison of activation and equilibrium thermodynamic parameters $\Delta \boldsymbol{H}^{\ddagger}$, $\Delta \boldsymbol{S}^{\ddagger}$, ΔH°, and ΔS°) for base-catalyzed aldose–ketose isomerization over different catalysts.

Reaction	Catalyst	$\Delta \boldsymbol{H}^{\ddagger}$(kJ mol^{-1})	$\Delta \boldsymbol{S}^{\ddagger}$ (J mol^{-1} K^{-1})	$\Delta \boldsymbol{H}^{\circ}$(kJ mol^{-1})	$\Delta \boldsymbol{S}^{\circ}$ (J mol^{-1} K^{-1})	$\Delta \boldsymbol{G}^{\circ}_{298}$ (kJ mol^{-1})	Ref
Glucose to fructose	Ti-Beta-F-155	108 ± 10	17 ± 26	n/a*	n/a	n/a	[113]
Glucose to fructose	Ti-Beta-OH-46	86 ± 9	-56 ± 26	n/a	n/a	n/a	[113]
Glucose to fructose	Et_3N	58 ± 8	-144 ± 30	n/a	n/a	n/a	[102]
Galactose to tagatose	Et_3N	48.7 ± 6	-181 ± 45	7.9 ± 5	21	1.64	This study
Tagatose to talose	Et_3N	75.4 ± 9	-111 ± 51	31.8 ± 18	75	9.45	This study

*n/a: Not available

3.4. Conclusions

This study quantified the kinetic and thermodynamic parameters governing the Et_3N-catalyzed isomerization of galactose to tagatose in aqueous medium. The reaction followed a reversible galactose–tagatose–talose network with parallel degradation, well described by a pseudo–first-order model across 40–100 °C. The forward rate constant of galactose to tagatose (k^{f}_{GT}) increased from 2.44 x 10^{-5} to 4.58 x 10^{-4} min^{-1}, with activation energies of 50.6 and 73.1 kJ mol^{-1} for the galactose–tagatose and tagatose–talose steps, respectively. Equilibrium analysis confirmed an endothermic, entropy-driven process (ΔH° = 7.9 and 31.8 kJ mol^{-1}; ΔS° = 21 J $mol^{-1}K^{-1}$). The established kinetic and thermodynamic framework enables quantitative prediction of

tagatose conversion and selectivity under various process conditions. The parameters obtained here can be directly applied to model reactor performance, optimize catalyst loading, and evaluate energy efficiency for large-scale rare-sugar manufacturing.

Future Perspective

While the findings presented in this thesis establish a robust chemical and process framework for the non-enzymatic production of D-tagatose, the transition from laboratory-scale experiments to industrial implementation requires addressing several multifaceted challenges. The observations regarding CaO-mediated isomerization and triethylamine-catalyzed kinetics provide a foundation, yet the potential for further optimization remains significant, particularly in the areas of mass transfer, mechanistic refinement, and systemic sustainability.

A primary constraint identified during the investigation of high-concentration galactose solutions (1.0 M) was the formation of a highly rigid and cohesive hydrogel complex. This dense crosslinked network, stabilized by Ca^{2+} coordination, effectively inhibited the diffusion of CO_2 during the neutralization step, rendering standard quenching methods ineffective. Future research should focus on the engineering of specialized reactor configurations, such as high-shear thin-film reactors or ultrasonic-assisted mixing systems, to disrupt the physical gel structure during carbonation. Furthermore, exploring the use of high-pressure CO_2 systems (>100 psi) could enhance gas solubility and penetration depth, potentially allowing the process to operate at higher substrate loadings without compromising the 86.65% conversion rates achieved at lower concentrations.

The current work utilizes kinetic modeling and stoichiometric substitution to infer the roles of OH^- and Ca^{2+} ions. However, a detailed molecular-level understanding of the Ca^{2+}-enediol coordination geometry remains an area for future exploration. Utilizing in-situ techniques such as High-Field Nuclear Magnetic Resonance (NMR) or X-ray Absorption Fine Structure (XAFS) could provide direct evidence of the specific hydroxyl groups involved in metal coordination. Quantifying the bond lengths and coordination numbers during the transition state would allow for the rational design of heterogeneous catalysts that mimic the local electronic environment of the calcium-sugar complex, potentially shifting the process from a stoichiometric reagent system to a true catalytic cycle.

From a sustainability standpoint, the LCA identified that CaO production is a major contributor to the environmental burden, accounting for 1.42 kg CO_2-eq/kg tagatose. To improve the ecological profile of this technology, future perspectives should include the development of a closed-loop system for calcium recovery. The precipitated $CaCO_3$ generated during CO_2 neutralization represents a high-purity byproduct. Research into low-temperature calcination methods or the direct utilization of this $CaCO_3$ in downstream pharmaceutical or construction applications could offset the environmental and economic costs of the primary reagents. Furthermore, validating this system using actual industrial streams, such as hydrolyzed whey permeate, is essential to determine the impact of residual dairy proteins and minerals on the forward rate constant and the overall tagatose selectivity.

The kinetic and thermodynamic parameters extracted from the Et_3N model provide the first quantitative framework for describing the reversible galactose-tagatose-talose network. This approach should be extended to other rare sugar systems, such as the isomerization of D-mannose to D-fructose or D-allose to D-psicose. Expanding the model to include the effects of varying ionic strengths and different solvent environments (e.g., aqueous-organic mixtures) would refine the predictive power of the Arrhenius and Eyring analyses. Such models are critical for the development of digital twins for rare sugar refineries, enabling real-time optimization of residence times to maximize tagatose yield while minimizing the irreversible degradation pathways identified at elevated temperatures (100 °C).

Conclusion

The research presented in this thesis establishes a comprehensive and sustainable non-enzymatic framework for the production of D-tagatose, addressing the critical global need for low-calorie sucrose alternatives. Through the integration of reaction system development, mechanistic investigation, and process-level evaluation, this work demonstrates that the chemical isomerization of D-galactose can be achieved with high efficiency and minimal environmental impact

A primary contribution of this study is the development of a CaO-mediated isomerization system that operates effectively under mild, room-temperature conditions. Experimental results revealed that a reaction utilizing a 0.5 M galactose solution with a 1/1 CaO/galactose molar ratio achieved a galactose conversion of 86.65% and a tagatose yield of 43.73% within a 30-min residence time. Mechanistic studies confirmed that CaO acts as a stoichiometric reagent rather than a traditional catalyst in this aqueous environment; hydroxide ions initiate the formation of reactive enediol intermediates, while Ca^{2+} ions provide essential stabilization through coordination with sugar hydroxyl groups.

The application of TEA and LCA provided critical insights into the industrial feasibility of the proposed technology. Among the neutralization strategies evaluated, CO_2 neutralization emerged as the most advantageous route. This process achieved a competitive MSP of $0.81/kg, which is significantly lower than current market prices for other rare sugars like allulose. Furthermore, the LCA demonstrated that sequestering CO_2 during the quenching step reduced the global warming potential to 0.90 kg CO_2-eq/kg tagatose, establishing this as a superior environmental alternative to mineral acid neutralization.

Finally, this work quantified the fundamental parameters governing the galactose isomerization network using a homogeneous triethylamine model. The study successfully modeled a reversible galactose–tagatose–talose network alongside parallel irreversible degradation pathways. Kinetic analysis showed that the forward rate constant for tagatose formation (k_{GT}^{f}) increased from 2.44×10^{-5} to 4.58×10^{-4} min^{-1} across a temperature range of 40–100 °C. Thermodynamic data ($\Delta H^{\circ} = 7.9$ kJ mol^{-1} and $\Delta S^{\circ} = 21$ J mol^{-1} K^{-1}) confirmed that the reaction is endothermic and entropy-driven, requiring moderate temperatures and controlled residence times to maximize yield.

In summary, this thesis bridges the gap between fundamental carbohydrate chemistry and industrial process design. By providing a quantitative and sustainable basis for non-enzymatic sugar isomerization, this research offers a scalable solution for the production of functional sweeteners to support global metabolic health.

References

[1] P.J. Rogers, The role of low-calorie sweeteners in the prevention and management of overweight and obesity: evidence v. conjecture, Proceedings of the Nutrition Society 77 (2018) 230–238. https://doi.org/10.1017/S0029665117004049.

[2] A.O. Musaiger, Overweight and obesity in Eastern Mediterranean Region: Prevalence and possible causes, J. Obes. 2011 (2011). https://doi.org/10.1155/2011/407237.

[3] S. Amarya, K. Singh, M. Sabharwal, Health consequences of obesity in the elderly, Journal of Clinical Gerontology and Geriatrics 5 (2014) 63–67. https://doi.org/10.1016/J.JCGG.2014.01.004.

[4] L. Poston, R. Caleyachetty, S. Cnattingius, C. Corvalán, R. Uauy, S. Herring, M.W. Gillman, Preconceptional and maternal obesity: epidemiology and health consequences, Lancet Diabetes Endocrinol. 4 (2016) 1025–1036. https://doi.org/10.1016/S2213-8587(16)30217-0.

[5] D. Mohajan, H.K. Mohajan, Obesity and Its Related Diseases: A New Escalating Alarming in Global Health, Journal of Innovations in Medical Research 2 (2023) 12–23. https://doi.org/10.56397/JIMR/2023.03.04.

[6] E.D. Parker, J. Lin, T. Mahoney, N. Ume, G. Yang, R.A. Gabbay, N.A. Elsayed, R.R. Bannuru, Economic costs of diabetes in the u.S. in 2022, Diabetes Care 47 (2024) 26–43. https://doi.org/10.2337/dci23-0085.

[7] J.R. Bober, N.U. Nair, Galactose to tagatose isomerization at moderate temperatures with high conversion and productivity, Nature Communications 2019 10:1 10 (2019) 4548-. https://doi.org/10.1038/s41467-019-12497-8.

[8] A. Drewnowski, C.D. Rehm, Socio-demographic correlates and trends in low-calorie sweetener use among adults in the United States from 1999 to 2008, Eur. J. Clin. Nutr. 69 (2015) 1035–1041. https://doi.org/10.1038/ejcn.2015.38.

[9] M. Kroger, K. Meister, R. Kava, Low-calorie sweeteners and other sugar substitutes: A review of the safety issues, Compr. Rev. Food Sci. Food Saf. 5 (2006) 35–47. https://doi.org/10.1111/j.1541-4337.2006.tb00081.x.

[10] M. Daher, C. Fahd, A.A. Nour, Y. Sacre, Trends and amounts of consumption of low-calorie sweeteners: A cross-sectional study, Clin. Nutr. ESPEN 48 (2022) 427–433. https://doi.org/10.1016/j.clnesp.2022.01.006.

[11] R.J. Johnson, L.G. Sánchez-Lozada, M.A. Lanaspa, The fructose survival hypothesis as a mechanism for unifying the various obesity hypotheses, Obesity 32 (2024) 12–22. https://doi.org/10.1002/OBY.23920;WGROUP:STRING:PUBLICATION.

[12] D.K. Oh, Tagatose: Properties, applications, and biotechnological processes, Appl. Microbiol. Biotechnol. 76 (2007) 1–8. https://doi.org/10.1007/s00253-007-0981-1.

[13] M. Guerrero-Wyss, S. Durán Agüero, L. Angarita Dávila, D-Tagatose Is a Promising Sweetener to Control Glycaemia: A New Functional Food, Biomed Res. Int. 2018 (2018). https://doi.org/10.1155/2018/8718053.

[14] J. Jayamuthunagai, P. Gautam, G. Srisowmeya, M. Chakravarthy, Biocatalytic production of D-tagatose: A potential rare sugar with versatile applications, Crit. Rev. Food Sci. Nutr. 57 (2017) 3430–3437. https://doi.org/10.1080/10408398.2015.1126550.

[15] S. Roy, J. Chikkerur, S.C. Roy, A. Dhali, A.P. Kolte, M. Sridhar, A.K. Samanta, Tagatose as a Potential Nutraceutical: Production, Properties, Biological Roles, and Applications, J. Food Sci. 83 (2018) 2699–2709. https://doi.org/10.1111/1750-3841.14358.

[16] P. Kim, Current studies on biological tagatose production using L-arabinose isomerase: A review and future perspective, Appl. Microbiol. Biotechnol. 65 (2004) 243–249. https://doi.org/10.1007/s00253-004-1665-8.

[17] C.M. Vastenavond, H. Bertelsen, S.J. Hansen, R.S. Laursen, J. Saunders, K. Eriknauer, Tagatose (D-tagatose), Alternative Sweeteners: Fourth Edition (2016) 197–221. https://doi.org/10.1201/B11242-16/TAGATOSE-TAGATOSE-CHRISTIAN-VASTENAVOND-HANS-BERTELSEN-S.

[18] Y. Lu, G. V. Levin, T.W. Donner, Tagatose, a new antidiabetic and obesity control drug, Diabetes Obes. Metab. 10 (2008) 109–134. https://doi.org/10.1111/j.1463-1326.2007.00799.x.

[19] O. Rojo-Poveda, L. Barbosa-Pereira, D. Orden, C. Stévigny, G. Zeppa, M. Bertolino, Physical Properties and Consumer Evaluation of Cocoa Bean Shell-Functionalized Biscuits Adapted for Diabetic Consumers by the Replacement of Sucrose with Tagatose, Foods 2020, Vol. 9, 9 (2020). https://doi.org/10.3390/foods9060814.

[20] D.D. Torrico, J. Tam, S. Fuentes, C.G. Viejo, F.R. Dunshea, D-Tagatose as a Sucrose Substitute and Its Effect on the Physico-Chemical Properties and Acceptability of Strawberry-Flavored Yogurt, Foods 2019, Vol. 8, 8 (2019). https://doi.org/10.3390/foods8070256.

[21] Z. Wang, Lobry de Bruyn-Alberda van Ekenstein Transformation, Comprehensive Organic Name Reactions and Reagents (2010) 1763–1766. https://doi.org/10.1002/9780470638859.CONRR396.

[22] P. Drabo, I. Delidovich, Catalytic isomerization of galactose into tagatose in the presence of bases and Lewis acids, Catal. Commun. 107 (2018) 24–28. https://doi.org/10.1016/j.catcom.2018.01.011.

[23] S. Babaei, N. Arabi, X. Shi, G.W. Huber, E. Camprubi, J. Zhao, Sustainable Production of Low-Calorie Tagatose via CaO-Promoted Galactose Isomerization with CO2 Neutralization under Ambient Conditions, Ind. Eng. Chem. Res. 64 (2025) 18656–18663. https://doi.org/10.1021/ACS.IECR.5C01664.

[24] C.A. Collyer, D.M. Blow, Observations of reaction intermediates and the mechanism of aldose-ketose interconversion by D-xylose isomerase, Proc. Natl. Acad. Sci. U. S. A. 87 (1990) 1362–1366. https://doi.org/10.1073/pnas.87.4.1362.

[25] A. Corma, H. García, Lewis Acids: From Conventional Homogeneous to Green Homogeneous and Heterogeneous Catalysis, Chem. Rev. 103 (2003) 4307–4365. https://doi.org/10.1021/cr030680z.

[26] A. Corma, L.T. Nemeth, M. Renz, S. Valencia, Sn-zeolite beta as a heterogeneous chemoselective catalyst for Baeyer–Villiger oxidations, Nature 2001 412:6845 412 (2001) 423–425. https://doi.org/10.1038/35086546.

[27] A. Corma, M.E. Domine, L. Nemeth, S. Valencia, Al-Free Sn-Beta Zeolite as a Catalyst for the Selective Reduction of Carbonyl Compounds (Meerwein−Ponndorf−Verley Reaction), J. Am. Chem. Soc. 124 (2002) 3194–3195. https://doi.org/10.1021/ja012297m.

[28] J. Zhao, Z. Wang, Q. Jin, D. Feng, J. Lee, Isomerization of Galactose to Tagatose: Recent Advances in Non-enzymatic Isomerization, J. Agric. Food Chem. 71 (2023) 4228–4234. https://doi.org/10.1021/acs.jafc.3c00095.

[29] H.S. El Khadem, S. Ennifar, H.S. Isbell, Contribution of the reaction pathways involved in the isomerization of monosaccharides by alkali, Carbohydr. Res. 169 (1987) 13–21. https://doi.org/10.1016/0008-6215(87)80238-0.

[30] D.M. Gao, T. Kobayashi, S. Adachi, Production of rare sugars from common sugars in subcritical aqueous ethanol, Food Chem. 175 (2015) 465–470. https://doi.org/10.1016/j.foodchem.2014.11.144.

[31] J. Dijkmans, D. Gabriëls, M. Dusselier, F. De Clippel, P. Vanelderen, K. Houthoofd, A. Malfliet, Y. Pontikes, B.F. Sels, Productive sugar isomerization with highly active Sn in dealuminated β zeolites, Green Chemistry 15 (2013) 2777–2785. https://doi.org/10.1039/c3gc41239c.

[32] K.B. Hicks, Ketose sugars from aldose sugars, 1981.

[33] T. Tanase, T. Takei, M. Hidai, S. Yano, Substrate-dependent chemoselective aldose–aldose and aldose–ketose isomerizations of carbohydrates promoted by a combination of calcium ion and monoamines, Carbohydr. Res. 333 (2001) 303–312. https://doi.org/10.1016/S0008-6215(01)00156-2.

[34] A. Cardelle-Cobas, N. Corzo, M. Villamiel, A. Olano, Isomerization of lactose-derived oligosaccharides: A case study using sodium aluminate, J. Agric. Food Chem. 56 (2008) 10954–10959. https://doi.org/10.1021/jf801952k.

[35] J.R.; S.J.P.; W.T.J. Beadle, Process for Manufacturing Tagatose, 1992. https://doi.org/https://patents.google.com/patent/US5078796A/en.

[36] Y. Xu, Process for Manufacturing Tagatose and Glucose, 2010. https://doi.org/https://patents.google.com/patent/US20130081613A1/en.

[37] B. Devi, S.M. Arumugam, S. Mahala, R.K. Kunchala, S. Elumalai, Galactose isomerization to tagatose over MgBr2 follows a temperature-dependent reaction rate kinetics as predicted by first principles-based theories, Molecular Catalysis 549 (2023). https://doi.org/10.1016/j.mcat.2023.113478.

[38] I.M. Abrams, J.R. Millar, Isomerization and epimerization of galactose using an anion exchange resin, Food and Bioproducts Processing 150 (2025) 151–158. https://doi.org/10.1016/s1381-5148(97)00058-8.

[39] N. Milasing, P. Khuwijitjaru, S. Adachi, Isomerization of galactose to tagatose using arginine as a green catalyst, Food Chem. 398 (2023). https://doi.org/10.1016/j.foodchem.2022.133858.

[40] P.S.J. Cheetham, A.N. Wootton, Bioconversion of d-galactose into d-tagatose, Enzyme Microb. Technol. 15 (1993) 105–108. https://doi.org/10.1016/0141-0229(93)90032-W.

[41] E. Troyano, I. Martinez-Castro, A. Olano, Kinetics of galactose and tagatose formation during heat-treatment of milk, Food Chem. 45 (1992) 41–43. https://doi.org/10.1016/0308-8146(92)90010-Y.

[42] M. Fischer, P. Drabo, I. Delidovich, Study of base-catalyzed isomerization of d-glucose with a focus on reaction kinetics, Reaction Kinetics, Mechanisms and Catalysis 135 (2022) 2357–2377. https://doi.org/10.1007/s11144-022-02277-9.

[43] G. Tofani, E. Jasiukaitytė-Grojzdek, M. Grilc, B. Likozar, Organosolv biorefinery: resource-based process optimisation, pilot technology scale-up and economics, Green Chemistry 26 (2024) 186–201. https://doi.org/10.1039/D3GC03274D.

[44] A. Filina, N. Jemaa, T. Saulnier-Bellemare, E. Bessède, C. Lecocq, M.C. Scaldaferri, S. Lefebvre, Techno-economic analysis (TEA) and life-cycle assessment (LCA) methodology as a tool for biorefining technology benchmarking and iterative process design, Biomass Bioenergy 204 (2026) 108390. https://doi.org/10.1016/J.BIOMBIOE.2025.108390.

[45] Obesity and overweight, Https://Www.Who.Int/News-Room/Fact-Sheets/Detail/Obesity-and-Overweight (n.d.).

[46] World Obesity Atlas 2024 | World Obesity Federation, (n.d.). https://www.worldobesity.org/news/world-obesity-atlas-2024 (accessed March 9, 2026).

[47] New weight-loss drugs surge in popularity amid obesity surge in US, worldwide | Pew Research Center, (n.d.). https://www.pewresearch.org/short-reads/2024/03/21/as-obesity-rates-rise-in-the-us-and-worldwide-new-weight-loss-drugs-surge-in-popularity/ (accessed March 9, 2026).

[48] Z.J. Ward, S.N. Bleich, M.W. Long, S.L. Gortmaker, Association of body mass index with health care expenditures in the United States by age and sex, PLoS One 16 (2021) e0247307. https://doi.org/10.1371/journal.pone.0247307.

[49] B. Masood, M. Moorthy, Causes of obesity: a review, Clinical Medicine 23 (2023) 284–291. https://doi.org/10.7861/CLINMED.2023-0168.

[50] E.S. van der Valk, E.L.T. van den Akker, M. Savas, L. Kleinendorst, J.A. Visser, M.M. Van Haelst, A.M. Sharma, E.F.C. van Rossum, A comprehensive diagnostic approach to detect underlying causes of obesity in adults, Obesity Reviews 20 (2019) 795–804. https://doi.org/10.1111/obr.12836.

[51] A.A. of P.S. on A. Health, AM:STARs: Obesity and Diabetes in the Adolescent, Vol. 28, No. 2, AM:STARs: Obesity and Diabetes in the Adolescent, Vol. 28, No. 2 (2017). https://doi.org/10.1542/9781581109405.

[52] M. Ashwell, S. Gibson, F. Bellisle, J. Buttriss, A. Drewnowski, M. Fantino, A.M. Gallagher, K. De Graaf, S. Goscinny, C.A. Hardman, H. Laviada-Molina, R. López-García, B. Magnuson, D. Mellor, P.J. Rogers, I. Rowland, W. Russell, J.L. Sievenpiper, C. La Vecchia, Expert consensus on low-calorie sweeteners: Facts, research gaps and suggested actions, Nutr. Res. Rev. 33 (2020) 145–154. https://doi.org/10.1017/S0954422419000283.

[53] M. Kroger, K. Meister, R. Kava, Low-calorie sweeteners and other sugar substitutes: A review of the safety issues, Compr. Rev. Food Sci. Food Saf. 5 (2006) 35–47. https://doi.org/10.1111/j.1541-4337.2006.tb00081.x.

[54] E. Moriconi, A. Feraco, V. Marzolla, M. Infante, M. Lombardo, A. Fabbri, M. Caprio, Neuroendocrine and Metabolic Effects of Low-Calorie and Non-Calorie Sweeteners, Front. Endocrinol. (Lausanne). 11 (2020) 525620. https://doi.org/10.3389/fendo.2020.00444.

[55] Allulose Market Size, Share & Growth | Industry Report 2034, Https://Www.Gminsights.Com/Industry-Analysis/Allulose-Market (n.d.).

[56] Allulose Market - Companies, Size, Share & Research Analysis, (n.d.). https://www.coherentmarketinsights.com/market-insight/allulose-market-492 (accessed March 9, 2026).

[57] A.M. Bolger, R.A. Rastall, M.J. Oruna-Concha, J. Rodriguez-Garcia, Effect of D-allulose, in comparison to sucrose and D-fructose, on the physical properties of cupcakes, LWT 150 (2021). https://doi.org/10.1016/j.lwt.2021.111989.

[58] E. Sokołowska, A. Sadowska, D. Sawicka, I. Kotulska-Bąblińska, H. Car, A head-to-head comparison review of biological and toxicological studies of isomaltulose, d-tagatose, and trehalose on glycemic control, Crit. Rev. Food Sci. Nutr. 62 (2022) 5679–5704. https://doi.org/10.1080/10408398.2021.1895057.

[59] GRAS Notices, (n.d.). https://hfpappexternal.fda.gov/scripts/fdcc/index.cfm?set=GRASNotices&id=977&sort=GRN_No&order=DESC&startrow=1&type=basic&search=911 (accessed March 9, 2026).

[60] A.C. Sylvetsky, K.I. Rother, Trends in the consumption of low-calorie sweeteners, Physiol. Behav. 164 (2016) 446–450. https://doi.org/10.1016/j.physbeh.2016.03.030.

[61] X. Zhang, R. Lu, Q. Wang, M. Hu, Z. Li, M. Xu, T. Yang, R. Zhang, Z. Rao, Production of d-Tagatose by Whole-Cell Conversion of Recombinant Bacillus subtilis in the Absence of Antibiotics, Biology 2021, Vol. 10, 10 (2021). https://doi.org/10.3390/biology10121343.

[62] H. Huang, C. Pandya, C. Liu, N.F. Al-Obaidi, M. Wang, L. Zheng, S.T. Keating, M. Aono, J.D. Love, B. Evans, R.D. Seidel, B.S. Hillerich, S.J. Garforth, S.C. Almo, P.S. Mariano, D. Dunaway-Mariano, K.N. Allen, J.D. Farelli, Panoramic view of a superfamily of phosphatases through substrate profiling, Proc. Natl. Acad. Sci. U. S. A. 112 (2015) E1974–E1983. https://doi.org/10.1073/pnas.1423570112.

[63] J.D. Thompson, K. Yamanaka, Thermostable isomerase and use hereof, in particular for producing tagatose, Appl. Microbiol Biotechnology 38 (2002) 403–413.

[64] S.K. Rai, H. Kaur, B.S. Kauldhar, S.K. Yadav, Dual-Enzyme Metal Hybrid Crystal for Direct Transformation of Whey Lactose into a High-Value Rare Sugar D-Tagatose: Synthesis, Characterization, and a Sustainable Process, ACS Biomater. Sci. Eng. 6 (2020) 6661–6670. https://doi.org/10.1021/acsbiomaterials.0c00841.

[65] D.W. Jeong, J.E. Hyeon, S.K. Shin, S.O. Han, Trienzymatic Complex System for Isomerization of Agar-Derived d-Galactose into d-Tagatose as a Low-Calorie Sweetener, J. Agric. Food Chem. 68 (2020) 3195–3202. https://doi.org/10.1021/acs.jafc.9b07536.

[66] Q. Guo, Y. An, J. Yun, M. Yang, T.A. Magocha, J. Zhu, Y. Xue, Y. Qi, Z. Hossain, W. Sun, X. Qi, Enhanced d-tagatose production by spore surface-displayed l-arabinose isomerase from isolated Lactobacillus brevis PC16 and biotransformation, Bioresour. Technol. 247 (2018) 940–946. https://doi.org/10.1016/j.biortech.2017.09.187.

[67] K. Izumori, A single and two step isomerization process for d-tagatose and l-ribose bioproduction using l-arabinose isomerase and d-lyxose isomerase, Enzyme Microb. Technol. 97 (2017) 27–33. https://doi.org/10.1016/j.jbiotec.2006.04.016.

[68] T.K. Nguyen, M.G. Hong, P.S. Chang, B.H. Lee, S.H. Yoo, Biochemical properties of L-arabinose isomerase from Clostridium hylemonae to produce D-tagatose as a functional sweetener, PLoS One 13 (2018) e0196099. https://doi.org/10.1371/journal.pone.0196099.

[69] X. Lü, S. Saka, New insights on monosaccharides' isomerization, dehydration and fragmentation in hot-compressed water, J. Supercrit. Fluids 61 (2012) 146–156. https://doi.org/10.1016/J.SUPFLU.2011.09.005.

[70] Y. Onishi, Y. Furushiro, S. Adachi, T. Kobayashi, Isomerization and Epimerization of Galactose to Tagatose and Talose in a Phosphate Buffer Containing Organic Solvents under Subcritical Water Conditions, Ind. Eng. Chem. Res. 60 (2021) 5084–5089. https://doi.org/10.1021/acs.iecr.1c00682.

[71] D.Y. Murzin, E. V. Murzina, A. Aho, M.A. Kazakova, A.G. Selyutin, D. Kubicka, V.L. Kuznetsov, I.L. Simakova, Aldose to ketose interconversion: Galactose and arabinose isomerization over heterogeneous catalysts, Catal. Sci. Technol. 7 (2017) 5321–5331. https://doi.org/10.1039/c7cy00281e.

[72] A. Cardelle-Cobas, N. Corzo, M. Villamiel, A. Olano, Isomerization of Lactose-Derived Oligosaccharides: A Case Study Using Sodium Aluminate, J. Agric. Food Chem. 56 (2008) 10954–10959. https://doi.org/10.1021/jf801952k.

[73] Z. Wang, M. Wang, X. Lyu, C. Wang, Y. Tong, X. Hua, R. Yang, Recycling preparation of high-purity tagatose from galactose using one-pot boronate affinity adsorbent-based adsorption-Assisted isomerization and simultaneous purification, Chemical Engineering Journal 446 (2022). https://doi.org/10.1016/j.cej.2022.137089.

[74] A.R.; K.O.M.; H.D.W.; S.D.; N.R.R. V. Oroskar, Tagatose Production Using Simulated Moving Bed Separation, 2014. https://doi.org/https://patents.google.com/patent/US8802843B2/en.

[75] J. Zhao, E. Cruz, X. Shi, S.A. Rankin, G.W. Huber, Production of Tagatose from Galactose with CaO at Room Temperature, ChemCatChem (2024). https://doi.org/10.1002/cctc.202401533.

[76] ISO 14044:2006, Https://Www.Iso.Org/Standard/38498.Html (n.d.). https://doi.org/(accessed 2025-04-02).

[77] Z. Guo, C.M. Pedersen, H. Chang, Y. Wang, Y. Qiao, Highly efficient production and purification of fructose via glucose isomerization by calcium chloride and triethylamine, Green Chemistry 25 (2023) 6297–6305. https://doi.org/10.1039/d3gc01141k.

[78] S.J. Angyal, The Lobry de Bruyn-Alberda van Ekenstein Transformation and Related Reactions, in: 2001: pp. 1–14. https://doi.org/10.1007/3-540-44422-x_1.

[79] I. Delidovich, Toward Understanding Base-Catalyzed Isomerization of Saccharides, ACS Catal. 13 (2023) 2250–2267. https://doi.org/10.1021/acscatal.2c04786.

[80] W. Zhang, S. Yu, T. Zhang, B. Jiang, W. Mu, Recent advances in d-allulose: Physiological functionalities, applications, and biological production, Trends Food Sci. Technol. 54 (2016) 127–137. https://doi.org/10.1016/j.tifs.2016.06.004.

[81] Y. Wang, H. Lim, The global childhood obesity epidemic and the association between socio-economic status and childhood obesity, International Review of Psychiatry 24 (2012) 176–188. https://doi.org/10.3109/09540261.2012.688195.

[82] Global Sugar Strategic Business Report 2023-2030 Featuring Associated British Foods, CJ CheilJedang, CSR, Hanseatische Zuckerraffinerie, Sudzucker, Syngenta, and Tate & Lyle, (n.d.). https://finance.yahoo.com/news/global-sugar-strategic-business-report-092100535.html (accessed October 25, 2025).

[83] P. Wang, S. Huang, R. Wang, X. Shi, H. Xu, J. Peng, Q. Chen, W. Zhang, L. Shi, X. Zhou, X. Tang, Global burden and cross-country inequalities in diseases associated with high body mass index from 1990 to 2019: Result from the Global Burden of Disease Study 2019, J. Glob. Health 14 (2024) 04200. https://doi.org/10.7189/jogh.14.04200.

[84] H. Sun, P. Saeedi, S. Karuranga, M. Pinkepank, K. Ogurtsova, B.B. Duncan, C. Stein, A. Basit, J.C.N. Chan, J.C. Mbanya, M.E. Pavkov, A. Ramachandaran, S.H. Wild, S. James, W.H. Herman, P. Zhang, C. Bommer, S. Kuo, E.J. Boyko, D.J. Magliano, IDF Diabetes Atlas: Global, regional and country-level diabetes prevalence estimates for 2021 and projections for 2045, Diabetes Res. Clin. Pract. 183 (2022). https://doi.org/10.1016/j.diabres.2021.109119.

[85] Diabetes, (n.d.). https://www.who.int/news-room/fact-sheets/detail/diabetes (accessed October 25, 2025).

[86] T. Oku, M. Okazaki, Laxative threshold of sugar alcohol erythritol in human subjects, . 16 (1996) 577–589. https://doi.org/10.1016/0271-5317(96)00036-X.

[87] G. V. Levin, Tagatose, the new GRAS sweetener and health product, J. Med. Food 5 (2002) 23–36. https://doi.org/10.1089/109662002753723197;REQUESTEDJOURNAL:JOURNAL:JMF

[88] G. Wang, X. Lyu, L. Wang, M. Wang, R. Yang, Highly efficient production and simultaneous purification of D-tagatose through one-pot extraction-assisted isomerization of D-galactose, Food Chem. X 20 (2023). https://doi.org/10.1016/j.fochx.2023.100928.

[89] K. Hashimoto, K. Sakaguchi, R. Kono, S. Adachi, Y. Watanabe, Isomerization and epimerization of galactose using an anion exchange resin, Food and Bioproducts Processing 150 (2025) 151–158. https://doi.org/10.1016/j.fbp.2025.01.010.

[90] P. Miao, Q. Wang, K. Ren, Z. Zhang, T. Xu, M. Xu, X. Zhang, Z. Rao, Advances and Prospects of d-Tagatose Production Based on a Biocatalytic Isomerization Pathway, Catalysts 13 (2023). https://doi.org/10.3390/catal13111437.

[91] J. Liu, X. Feng, L. Liang, L. Sun, D. Meng, Enzymatic biosynthesis of D-galactose derivatives: Advances and perspectives, Int. J. Biol. Macromol. 267 (2024) 131518. https://doi.org/10.1016/J.IJBIOMAC.2024.131518.

[92] S.L. Baptista, A. Romaní, C. Oliveira, S. Ferreira, C.M.R. Rocha, L. Domingues, Galactose to tagatose isomerization by the L-arabinose isomerase from Bacillus subtilis: A biorefinery approach for Gelidium sesquipedale valorisation, LWT 151 (2021). https://doi.org/10.1016/j.lwt.2021.112199.

[93] P. Torres, F. Batista-Viera, Production of d-tagatose and d-fructose from whey by co-immobilized enzymatic system, Molecular Catalysis 463 (2019) 99–109. https://doi.org/10.1016/J.MCAT.2018.11.017.

[94] F. Jørgensen, O.C. Hansen, P. Stougaard, Enzymatic conversion of D-galactose to D-tagatose: Heterologous expression and characterisation of a thermostable L-arabinose isomerase from Thermoanaerobacter mathranii, Appl. Microbiol. Biotechnol. 64 (2004) 816–822. https://doi.org/10.1007/S00253-004-1578-6/FIGURES/3.

[95] Z. Xu, Z. Xu, B. Tang, S. Li, J. Gao, B. Chi, H. Xu, Construction and co-expression of polycistronic plasmids encoding thermophilic l-arabinose isomerase and

hyperthermophilic β-galactosidase for single-step production of d-tagatose, Biochem. Eng. J. 109 (2016) 28–34. https://doi.org/10.1016/J.BEJ.2015.12.015.

[96] N. Rajabbeigi, A.I. Torres, C.M. Lew, B. Elyassi, L. Ren, Z. Wang, H. Je Cho, W. Fan, P. Daoutidis, M. Tsapatsis, On the kinetics of the isomerization of glucose to fructose using Sn-Beta, Chem. Eng. Sci. 116 (2014) 235–242. https://doi.org/10.1016/J.CES.2014.04.031.

[97] G. Li, E.A. Pidko, E.J.M. Hensen, Synergy between Lewis acid sites and hydroxyl groups for the isomerization of glucose to fructose over Sn-containing zeolites: a theoretical perspective, Catal. Sci. Technol. 4 (2014) 2241–2250. https://doi.org/10.1039/C4CY00186A.

[98] Q. Yang, M. Sherbahn, T. Runge, Basic Amino Acids as Green Catalysts for Isomerization of Glucose to Fructose in Water, ACS Sustain. Chem. Eng. 4 (2016) 3526–3534. https://doi.org/10.1021/acssuschemeng.6b00587.

[99] N. Milasing, V. Toussaint, C. Hametner, P. Khuwijitjaru, I. Delidovich, Enhanced catalytic activity of carbonate buffer for isomerization of D-galactose into D-tagatose, Food Chem. 476 (2025) 143398. https://doi.org/10.1016/J.FOODCHEM.2025.143398.

[100] J.C. Speck, The Lobry De Bruyn-Alberda Van Ekenstein Transformation, Adv. Carbohydr. Chem. 13 (1958) 63–103. https://doi.org/10.1016/S0096-5332(08)60352-5.

[101] I. Delidovich, R. Palkovits, Catalytic Isomerization of Biomass-Derived Aldoses: A Review, ChemSusChem 9 (2016) 547–561. https://doi.org/10.1002/cssc.201501577.

[102] J.M. Carraher, C.N. Fleitman, J.P. Tessonnier, Kinetic and mechanistic study of glucose isomerization using homogeneous organic brønsted base catalysts in water, ACS Catal. 5 (2015) 3162–3173. https://doi.org/10.1021/acscatal.5b00316.

[103] S. Babaei, N. Arabi, J. Zhao, A Critical Review of Catalytic Glucose-to-Fructose Isomerization, ChemistrySelect 10 (2025) e05344. https://doi.org/10.1002/SLCT.202505344;WEBSITE:WEBSITE:CHEMISTRY-EUROPE;ISSUE:ISSUE:DOI.

[104] W. Wang, H. Ihara, Z. Yu, O.Z. Dziedzic, X. Shi, J.R. Featherman, A. Oroskar, S.A. Rankin, G.W. Huber, Tagatose Production from Dairy Waste: Chemical Isomerization and Process Economics, ACS Sustain. Chem. Eng. 13 (2025) 15493–15508. https://doi.org/10.1021/ACSSUSCHEMENG.5C05750.

[105] P. V. Danckwerts, The reaction of CO2 with ethanolamines, Chem. Eng. Sci. 34 (1979) 443–446. https://doi.org/10.1016/0009-2509(79)85087-3.

[106] H. Huang, X.G. Meng, W.W. Yu, L.Y. Chen, Y.Y. Wu, High Selective Isomerization of Glucose to Fructose Catalyzed by Amidoximed Polyacrylonitrile, ACS Omega 6 (2021) 19860–19866. https://doi.org/10.1021/acsomega.1c02577.

[107] M. Moliner, Y. Román-Leshkov, M.E. Davis, Tin-containing zeolites are highly active catalysts for the isomerization of glucose in water, Proc. Natl. Acad. Sci. U. S. A. 107 (2010) 6164–6168. https://doi.org/10.1073/pnas.1002358107.

[108] J. Tang, X. Guo, L. Zhu, C. Hu, Mechanistic Study of Glucose-to-Fructose Isomerization in Water Catalyzed by [Al(OH)2(aq)]+, ACS Catal. 5 (2015) 5097–5103. https://doi.org/10.1021/acscatal.5b01237.

[109] C. Kooyman, K. Vellenga, H.G.J. De Wilt, The isomerization of d-glucose into d-fructose in aqueous alkaline solutions, Carbohydr. Res. 54 (1977) 33–44. https://doi.org/10.1016/S0008-6215(77)80003-7.

[110] F. Yang, Q. Xia, G. Lin, Y. Su, W. Lin, H. Zhang, G. Liang, Isomerization of glucose to fructose catalyzed by MgCl2 in water, Fuel 379 (2025). https://doi.org/10.1016/j.fuel.2024.132985.

[111] Q. Hou, M.L.U. Rehman, X. Bai, C. Xie, R. Lai, H. Qian, T. Xia, G. Yu, Y. Tang, H. Xie, M. Ju, Incorporation of MgO into nitrogen-doped carbon to regulate adsorption for near-equilibrium isomerization of glucose into fructose in water, Appl. Catal. B 342 (2024). https://doi.org/10.1016/j.apcatb.2023.123443.

[112] Y.J. Zheng, K.M. Merz, G.K. Farber, Theoretical examination of the mechanism of aldose–ketose isomerization, Protein Eng. 6 (1993) 479–484. https://doi.org/10.1093/PROTEIN/6.5.479.

[113] M. Cordon, J.W. Harris, J.C. Vega-Vila, J.S. Bates, S. Kaur, M. Gupta, M.E. Witzke, E.C. Wegener, J.T. Miller, D.W. Flaherty, D.D. Hibbitts, R. Gounder, Dominant Role of Entropy in Stabilizing Sugar Isomerization Transition States within Hydrophobic Zeolite Pores, J. Am. Chem. Soc. 140 (2018) 14244–14266. https://doi.org/10.1021/JACS.8B08336.